

Evaluating Performance of Media Filters to Remove Phosphorus in Stormwater Pond



November 2023

Prepared by: Stone Environmental, Inc.
Dave Braun & Meghan Arpino

For:
The Lake Champlain Basin Program and NEIWPC

This report was funded and prepared under the authority of the Lake Champlain Special Designation Act of 1990, P.L. 101-596 and subsequent reauthorization in 2002 as the Daniel Patrick Moynihan Lake Champlain Basin Program Act, H. R. 1070, through the US EPA. Publication of this report does not signify that the contents necessarily reflect the views of the states of New York and Vermont, the Lake Champlain Basin Program, the US EPA or the Great Lakes Fishery Commission.

The Lake Champlain Basin Program has funded more than 100 technical reports and research studies since 1991. For complete list of LCBP Reports please visit:

<https://www.lcbp.org/news-and-media/publications/technical-reports/>

NEIWPCC Job Code: 0100-328-002

LCBP Project Code: L-2019-105



FINAL REPORT

NEIW PCC Job Cost Code: 0100-328-002
Project Code: L-2019-105
Contractor: Stone Environmental, Inc.
Prepared By: Dave Braun & Meghan Arpino
Contract Execution Date: 2/10/2020
Contract End Date: 12/30/2023
Date Submitted: 6/30/2023
Date Approved: 11/17/2023

EVALUATING PERFORMANCE OF MEDIA FILTERS TO REMOVE PHOSPHORUS IN STORMWATER POND OUTFLOW

CONTACT INFORMATION

Stone Environmental, Inc.
535 Stone Cutters Way, Montpelier, Vermont 05602
802-272-8819, Dbraun@stone-env.com

This project was funded by an agreement awarded by EPA to NEIWPCC in partnership with LCBP.

Although the information in this document may have been funded wholly or in part by the United States Environmental Protection Agency, it has not undergone the Agency's publications review process and therefore, may not necessarily reflect the views of the Agency and no official endorsement should be inferred.

The viewpoints expressed here do not necessarily represent those of LCBP, NEIWPCC, EPA, or the Great Lakes Fishery Commission, nor does mention of trade names, commercial products, or causes constitute endorsement or recommendation for use.

Executive Summary

Stone Environmental, Inc. (Stone) designed, constructed, and monitored four media filters to remove phosphorus (P) from the outflow of the Dorset Park stormwater pond in South Burlington, Vermont. This successful practice demonstration should encourage and inform the development of additional P filter retrofits to stormwater ponds in the Lake Champlain Basin.

The City of South Burlington assisted Stone in identifying a suitable stormwater pond for this study and advised Stone on the filter design. In December 2021, Stone and a hired contractor constructed four P filters in cells excavated in the bank of the Dorset Park stormwater pond. The filters are essentially identical except for the filter media. While the primary component of each filter is ½-inch diameter crushed shale, P sorbing amendments were blended with the crushed shale in three of the filters. The fourth (unamended) filter served as a control. Pond water enters at the base of each filter through a perforated pipe and flows laterally and up through the media into a perforated collection pipe installed at lower elevation than the pond's lowest outlet. Treated water flows by gravity from the collection pipe to the pond outlet structure. Overall, the hydraulic design of these filters was successful.

The filter containing ~8% dewatered drinking water treatment residuals significantly reduced concentrations of dissolved P (32%) and total P (41%). The filter containing zero-valent iron shavings removed a higher percentage of the dissolved and total phosphorus than the other three filters, reducing concentrations about 52%. Therefore, in similar P filter applications we recommend use of zero-valent iron. P concentration reduction was strongly dependent on inflow P concentration. Relatively low P concentrations in the inflow (median ~95 µg/L TP and ~60 µg/L TDP) resulted in somewhat lower P concentration reduction efficiency than we were expecting.

The filter containing activated alumina granules performed very poorly. It did not significantly reduce P and appeared to depress pH to unacceptable levels. In similar applications we recommend against the use of activated alumina. Finally, the filter containing only crushed black shale did not significantly reduce P, and actually released P during summer low-flow conditions.

Implementation of media filters to enhance P removal at existing stormwater ponds can reduce P loading to the receiving water. Stormwater ponds having relatively high outflow P concentrations and outlet structures suitable for modification are most suitable for implementing this type of P filter retrofit. Stone ensured that the results provided by this study are suitable for establishing a P reduction crediting method for filter retrofit practices. Establishing a transparent P reduction crediting method will provide MS4s and other potential permittees in the Lake Champlain Basin with an incentive to apply this retrofit practice.

Evaluating Performance of Media Filters to Remove Phosphorus in Stormwater Pond

Contents

Executive Summary	3
1. Introduction	8
1.1. Background	8
1.2. Current Project.....	9
1.3. Project Objectives	9
2. Tasks Completed	10
3. Methods	11
3.1. P Filter Design	11
3.2. P Filter Construction.....	11
3.2.1. Filter media	13
3.2.2. Filter construction cost.....	14
3.3. Installation of Monitoring Systems	14
3.4. Monitoring Filter Outflows.....	15
3.5. Water Sample Analysis.....	15
3.6. Challenges Encountered.....	16
4. Quality Assurance Tasks Completed	17
5. Phosphorus Filter Results	19
5.1. Summary of Water Quality, Flow Rate, and P Loading Data at Inflows and Outflows.....	19
5.1.1. Water quality parameters	22
5.1.2. Flow rates.....	25
5.1.3. TP and TDP concentrations	26
5.1.4. TP and TDP loading.....	28
5.1.5. TP and TDP concentration timeseries.....	30
5.2. P Filter Performance	33
5.2.1. Simple linear regressions on inflow/outflow P concentrations	35
5.2.2. Simple linear regressions on inflow/outflow P loads.....	37
5.2.3. Simple linear regressions of percent reduction on inflow P concentration	40
5.2.4. Filter performance relative to flow rate	43
5.2.5. Cumulative TP and TDP flux over the monitoring period	45
5.3. P Reduction Crediting.....	46
5.4. P Filter Design Improvements	47
5.5. Recommendations Regarding Implementation of P Filter Retrofits.....	47
6. Conclusions	49
7. Deliverables Completed	50
8. References	51

Appendix A: Quality Assurance Project Plan.....	53
Appendix B: Interim Report on Stormwater Pond Evaluation	54
Appendix C: As-Built P Filter Drawings	55
Appendix D: Flow and Water Quality Monitoring Data	56

Table of Figures

Figure 1. Installing perforated distribution pipe in Filter F _{AA}	12
Figure 2. Raking top of media bed	12
Figure 3. Filter media used in Dorset Park stormwater pond P filters	13
Figure 4. Sample collection	15
Figure 5. Distributions of temperature at filter inflows and outflows	23
Figure 6. Distributions of pH at filter inflows and outflows	24
Figure 7. Distributions of specific conductivity at filter inflows and outflows	25
Figure 8. Distributions of TP concentrations at filter inflows and outflows	27
Figure 9. Distributions of TDP concentrations at filter inflows and outflows	28
Figure 10. Distributions of TP loading rates at filter inflows and outflows	29
Figure 11. Distributions of TDP loading rates at filter inflows and outflows	30
Figure 12. TP concentration timeseries at filter inflows and outflows	31
Figure 13. TDP concentration timeseries at filter inflows and outflows	32
Figure 14. TP and TDP concentration distributions at filter intakes by season	33
Figure 15. Regression of F _{AA} inflow/outflow TP (left) and TDP (right) concentrations	35
Figure 16. Regression of F _{SBS} inflow/outflow TP (left) and TDP (right) concentrations	36
Figure 17. Regression of F _{DWTR} inflow/outflow TP (left) and TDP (right) concentrations	36
Figure 18. Regression of F _{ZVI} inflow/outflow TP (left) and TDP (right) concentrations	37
Figure 19. Regression of F _{AA} inflow/outflow TP (left) and TDP (right) loading	38
Figure 20. Regression of F _{SBS} inflow/outflow TP (left) and TDP (right) loading	38
Figure 21. Regression of F _{DWTR} inflow/outflow TP (left) and TDP (right) loading	39
Figure 22. Regression of F _{ZVI} inflow/outflow TP (left) and TDP (right) loading	39
Figure 23. Percent reduction of inflow TP (left) and TDP (right) concentrations at F _{AA}	41
Figure 24. Percent reduction of inflow TP (left) and TDP (right) concentrations at F _{SBS}	41
Figure 25. Percent reduction of inflow TP (left) and TDP (right) concentrations at F _{DWTR}	42
Figure 26. Percent reduction of inflow TP (left) and TDP (right) concentrations at F _{ZVI}	42
Figure 27. Percent reduction of inflow TP concentrations grouped by flow strata	44
Figure 28. Percent reduction of inflow TDP concentrations grouped by flow strata	45

Table of Tables

Table 1. Filter composition.....	14
Table 2. Filter construction costs	14
Table 3. Water analysis methods	16
Table 4. Summary of invalid TP and TDP data	18
Table 5. Descriptive statistics for F_{AA} inflows	20
Table 6. Descriptive statistics for F_{SBS} inflows.....	20
Table 7. Descriptive statistics for F_{DWTR} inflows	20
Table 8. Descriptive statistics for F_{ZVI} inflows	21
Table 9. Descriptive statistics for F_{AA} outflows	21
Table 10. Descriptive statistics for F_{SBS} outflows	21
Table 11. Descriptive statistics for F_{DWTR} outflows.....	22
Table 12. Descriptive statistics for F_{ZVI} outflows.....	22
Table 13. P-values from Wilcoxon rank sum tests between filter inflows and outflows ¹	34
Table 14. Percent reductions in P concentrations between filter inflows and outflows	34
Table 15. P concentration and load reduction estimates from linear regression equations	40
Table 16. P flux in filter inflows and outflows	46

1. Introduction

1.1. Background

Lake Champlain (Vermont – New York – Quebec) continues to suffer from the effects of excessive phosphorus (P) loading from sources in the Lake Champlain Basin (LCB). While stormwater ponds are not considered major sources of P in the LCB, some stormwater ponds present opportunities to enhance P removal. The primary limitations to enhancing P removal in stormwater ponds are that peak outflow rates are typically high and outflow P concentrations tend to be low; median concentrations of 90 µg/L total P (TP) and 60 µg/L total dissolved P (TDP) are reported in the International Best Management Practices Database (Clary et al, 2017). Since water column P concentrations tend to be low, chemical addition to coagulate and flocculate P is rarely attempted. However, Stone hypothesized that packed bed filters containing an appropriate P sorbing media could remove enough P from pond outflows to justify their cost of installation and maintenance.

Enhancing the P removal of stormwater ponds using media filters could be a cost-effective management practice. Where P concentrations in outflows are typical, the cumulative amount of P removed by filters could still be significant if large volumes of water are treated over time. Greater benefits should be found where outflows have elevated P concentrations, because the P removal efficiency of filters tends to be higher when influent P concentrations are high. Certain, primarily older stormwater ponds have been shown to have substantially higher dissolved P outflow concentrations than the median concentrations reported in Clary et al. (2017). In a study of 98 Minnesota stormwater ponds, Gulliver (2018) reported that 32% of monitored ponds appeared to be net sources of P. Internal release of P from sediment under anoxic conditions resulted in substantially elevated P concentrations in the outflow.

In several respects, existing stormwater ponds can be ideal facilities for filter-based retrofit practices that enhance P removal. Stormwater ponds generally have enough land area surrounding the pond to construct P filters in the pond bank. They are often fenced, reducing the risk of vandalism. Municipal or contracted staff already maintaining the ponds could also maintain filter components. While some stormwater ponds are not suitable due to the configuration of their outlet structures, at others the elevation difference between the pond surface and the invert of the outlet structure can be exploited to operate gravity-flow filters.

Stormwater pond outflows are similar in some respects to agricultural tile drain flows. Flow rates and volumes tend to be high, while suspended solids and dissolved P concentrations are generally low, at least relative to surface runoff concentrations. P removal systems installed at the outlets of tile drains that direct flow through filtering media can significantly reduce P loads to drainage ditches and receiving waters (McDowell et al. 2008, Penn et al. 2012, Bryant et al. 2012). Stone previously designed two types of media filters to remove P from tile drain flow (Braun 2023, Braun 2017). In the present study, we applied our knowledge from this tile drain

work to a new and different application, treatment of stormwater pond outflow.

1.2. Current Project

In this demonstration study, Stone designed, constructed, and monitored four media filters to remove P from outflows of the Dorset Park stormwater pond in South Burlington, Vermont. We selected this pond for the study in consultation with the City of South Burlington's Stormwater Services Department from among 11 stormwater ponds we assessed in South Burlington. The primary pond selection criteria were relatively high TDP concentrations, reasonable access, and appropriate pond characteristics including bank height and slope and outlet configuration. Considering these factors, Stone and the City of South Burlington determined that the Dorset Park stormwater pond was the most appropriate pond for installation and testing of P filters.

The Dorset Park stormwater pond discharges to a tributary of Potash Brook. The area draining to the pond is quite large (~21 ha) and the pond itself is also large (0.4 ha). This is an advantage from a P removal standpoint, since over an annual cycle the filters should treat more water than filters installed on a small pond. However, because this project was an experiment and a demonstration study rather than a full-scale treatment practice, the P filters we designed for the Dorset Park stormwater pond are much too small to treat all its outflow. The proportion of the outflow that is treated may be lower than with a pond having a smaller drainage area.

The stormwater pond P filter design is intended for use by municipal stormwater managers. South Burlington municipal staff advised project staff regarding the filter design. In consultation with Vermont DEC, the City of South Burlington and Stone are pursuing a P reduction crediting method for this treatment practice. Establishing such a method will provide an incentive to apply this practice. This will be particularly true for municipalities and non-traditional entities subject to MS4 (Municipal Separate Storm Sewer System) permit requirements.

This project addresses multiple objectives and strategies outlined in *Opportunities for Action*. We demonstrated a strategy for reducing P pollution to Lake Champlain from urban stormwater by retrofitting a municipal stormwater pond with media filters to remove dissolved P (*Opportunities for Action* Task I.A.1.c). The study also provided critical data to quantify the performance of four different types of media in enhancing P removal at existing stormwater ponds.

1.3. Project Objectives

The two main study objectives were:

1. To design a cost-effective filter that can be used in retrofitting existing stormwater ponds to remove P from pond outflow.
2. To compare four types of filter media relative to their cost and capacity to remove P from stormwater pond outflow.

2. Tasks Completed

The following tasks were accomplished to meet the study objectives.

Prepare Quality Assurance Project Plan (QAPP): A primary data QAPP addressing the monitoring phases of the project was approved on July 16, 2020. This QAPP is included as Appendix A.

Evaluate Stormwater Ponds: In consultation with the City of South Burlington, 11 stormwater ponds in South Burlington were sampled to identify a pond with relatively high TDP concentrations in its outflow. Based on the measured TDP concentrations and engineering considerations, Stone and the City of South Burlington selected the Dorset Park stormwater pond as the most appropriate for installation and testing of P filters. This task was described in a technical memo, included as Appendix B.

Design P Filters: Stone prepared engineering plans for construction of P filters at the Dorset Park stormwater pond. This task is described in Section 3.1. The as-built filter drawings are included as Appendix C.

Construct P Filters: Stone oversaw construction of the P filters by Hebert Excavation. Stone provided the materials. Construction was completed by December 17, 2021, and the disturbed area was seeded and mulched on December 18, 2021. This task is described in Section 3.2.

Install Monitoring Systems: Stone completed installation of the flowmeters and sampling access points on December 17, 2021. This task is described in Section 3.3.

Monitor Filter Outflows: Stone collected the first set of samples and measured water quality parameters on March 18, 2022, and continued monitoring filter inflows and outflows weekly through mid-December 2022. Samples were analyzed for TP and TDP concentrations by the Vermont Agriculture and Environmental Laboratory (VAEL). Final flow and water quality data are included as Appendix D.

Analyze Data and Present Results: Stone tabulated flow data, field measurements, and analytical data as it was received. We submitted quarterly progress reports throughout the project term. We also submitted a technical memo (Appendix B) describing the stormwater pond evaluation. This final report covers aspects of design and construction of the P filters and presents the water quality data and an evaluation of the P filter performance.

3. Methods

3.1. P Filter Design

Stone designed four filters to remove P from the outflow of the Dorset Park stormwater pond. Each filter contains different media, but they are otherwise essentially identical. In the design phase Stone applied aspects of our prior work on agricultural tile drains (Braun 2023, Braun 2017) to treatment of stormwater pond outflow. While the media characteristics we seek (moderate to high hydraulic conductivity, good P sorption capacity, and low cost) are similar in both applications, there were marked differences in the filter design. Developing a filter design suitable for installation at existing stormwater ponds was a primary impetus for this project, in addition to continuing evaluation of potential filter media.

Belden and Fossum (2018) implemented P filters at a stormwater pond in Minnesota, with encouraging results. Rather than designing downflow filters, as did Belden and Fossum, Stone designed lateral/up-flow filters built into the sloping pond bank. Anticipated flow rates, media hydraulic conductivity, water residence time, and practical filter size were fundamental considerations in the filter design process. We sought to treat as much water as possible within a relatively small footprint, while ensuring adequate contact time of water in the media.

An elevation survey of the stormwater pond outlet structure was completed in April 2021. Stone used these data to prepare plans suitable for construction of the P filters. We received and addressed comments on these plans from the City of South Burlington (Dave Wheeler). Stone also made refinements in the P filter design following input from Hebert Excavation, the hired excavation contractor, to improve constructability given the challenging site conditions. The as-built P filter plans are included in Appendix C.

Since this project was a demonstration study with a small construction budget, the filter cells we designed are smaller than they would be in a full-scale stormwater pond retrofit. We did not attempt to treat all the outflow. In full-scale pond retrofits, we envision media filters could be installed around most of a pond's perimeter. It should be possible to make reasonable extrapolations from the resulting filter performance data to the scale of an entire stormwater pond based on the unit length of the filter cells.

3.2. P Filter Construction

Stone oversaw construction of the P filters and associated components by Hebert Excavation. The pond was drawn down to enable construction of the filters. Materials were assembled on site and structures were installed at predetermined elevations. Construction was completed by December 17, 2021, and the disturbed area was seeded and mulched on December 18, 2021.

The four P filters were constructed in a row aligned with the pond outlet structure (Appendix C). The filters were built in plywood boxes lined with 10-mil plastic sheeting (Figure 1). The plywood boxes are not structural; they were needed to prevent tearing of the plastic sheeting during

construction. Each filter is approximately 10 feet wide (axis parallel with the pond edge) and 7 feet long and is filled with approximately 6 cubic yards of the assigned media (see Section 3.2.1). Two 6-inch diameter, perforated intake pipes convey pond water into the filters. These pipes angle horizontally into the pond, close to the pond bottom. Intake “IN1” conveys pond water to filters F_{AA} and F_{SBS} , and intake “IN2” conveys water to filters F_{DWTR} and F_{ZVI} .

In each filter, a 6-inch diameter, perforated distribution pipe (Figure 1) was installed close to the bottom of the excavation, horizontal and spanning the long axis of the filter. The filter cell was partially filled with media, covering the distribution pipe. On the opposite side of the filter, a second perforated pipe, a 4-inch diameter collection pipe, was installed parallel to the distribution pipe. The collection pipe was installed at a slightly lower elevation (0.5 ft.) than the pond’s low flow offices. The distribution and collection pipes were set 6 ft. apart laterally and 0.8 ft. apart vertically. More media was added, covering the collection pipe by several inches

(Figure 2). When filled, pond water flows from the distribution pipe laterally and up through the media into the collection pipe. From the collection pipe, the treated water flows via gravity through 4-inch solid pipe to a monitoring manhole and then to the pond outlet structure.

In a permanent installation where monitoring is not needed, the perforated collection pipe could be connected directly to the pond outlet structure, similar to the design of the gravel outlet trench shown in Figure 4-21 of the 2017 Vermont Stormwater Management Manual (VSMM) (VANR 2017). This concept has the additional benefit of cooling pond water prior to discharge, in keeping with the 2017 VSMM requirements for new retention ponds discharging to surface waters designated as cold-water fisheries.



Figure 1. Installing perforated distribution pipe in Filter F_{AA}



Figure 2. Raking top of media bed

3.2.1. Filter media

Stone considered cost, predicted P sorption capacity, hydraulic properties, and necessary preparation in specifying the filter media. We used crushed Swanton black shale (SBS) in each filter because it is a locally available, inexpensive stone with acceptable hydraulic properties and some capacity to remove P. In Stone's St. Albans tile drain P filter study (Braun 2023), the filter containing SBS reduced TP and TDP concentrations by approximately 40 percent. As in the St. Albans study, the SBS used in the stormwater pond filters was graded to 1/2-inch by screening the crushed stone between 9/16-inch and 7/16-inch screens, removing most fines. This material was generously donated from the Swanton Limestone quarry by Rock Dust Local, a private company based in Bridport, Vermont.

The SBS was amended with three P sorbing materials, 3/16-inch activated alumina (AA) granules, alum-based drinking water treatment residuals (DWTR), or zero-valent iron shavings (ZVI). Figure 3 shows these materials. In Stone's St. Albans tile drain filter study, a blend of 90% SBS, 8% AA, and 2% ZVI reduced TP concentrations by 61% and TDP concentrations by 65% (Braun 2023). Stone obtained the AA from Delta Adsorbents (Roselle, IL) and ZVI shavings from Connelly GPM (Chicago, IL). We harvested dewatered DWTR for this study directly from the drying sheds at the Champlain Water District in South Burlington, Vermont. DWTR has been demonstrated to be an effective P sorbent in multiple studies, including Stone's first tile drain filter study in Franklin, Vermont (Braun 2017), although the material is quite fine and therefore prone to clogging.



Figure 3. Filter media used in Dorset Park stormwater pond P filters

The media types were randomly assigned to one of four filters. This side-by-side comparison provided information about the performance of crushed SBS alone and in combination with P sorbing amendments. Table 1 presents the composition of each filter by volume.

Table 1. Filter composition

Filter	Swanton Black Shale		Amendment				
	Cubic yards	Volume %	Type	Quantity	Density (lb./ft ³)	Cubic yards	Volume %
F _{AA}	5.4	86.4	AA (3/16" F-200)	1100 lb.	48	0.85	13.6
F _{SBS}	6.0	100.0	None	NA	NA	NA	NA
F _{DWTR}	5.4	92.5	DWTR	88 gal.	NA	0.44	7.5
F _{ZVI}	5.4	92.4	ZVI (ETI CC-1107)	1800 lb.	150	0.44	7.6

3.2.2. Filter construction cost

The total cost of constructing the four filters was \$26,260, excluding engineering (Table 2). In this cost comparison, the total costs of construction and materials were divided by four since these costs were essentially the same for each filter.

Table 2. Filter construction costs

Filter	Media type	Media and shipping	Pipe, fittings, misc.	Construction	Total
F _{AA}	SBS + AA	\$2,086	\$550	\$5,000	\$7,636
F _{SBS}	SBS only	\$155	\$550	\$5,000	\$5,705
F _{DWTR}	SBS + DWTR	\$155	\$550	\$5,000	\$5,705
F _{ZVI}	SBS + ZVI	\$1,664	\$550	\$5,000	\$7,214
Total					\$26,260

3.3. Installation of Monitoring Systems

A monitoring manhole was installed between the P filters and the pond outlet structure, and the filter outlet pipes were routed through the manhole. Within the manhole, a 2-inch diameter Zenner ZSU ultrasonic flowmeter was installed on each filter outlet pipe to continually measure flow rate. Our paramount consideration in selecting the Zenner ZSU ultrasonic flowmeters for this study was their outstanding accuracy at relatively low flow rates. The Zenner ZSU ultrasonic flowmeters were factory calibrated and did not require calibration for the duration of the study. The flowmeters cannot be calibrated in the field.

A pipe trap was installed downstream of each flowmeter to ensure full-pipe flow conditions for accurate flow measurement. Each filter outlet pipe was equipped with a gate valve for controlling flow rate. The filter outlet pipes were then routed to the pond outlet structure through 2.5-inch diameter holes cored in the side of the concrete structure.

A sampling port with dedicated tubing was installed on each filter outlet pipe to enable sample collection using a portable peristaltic pump. A solar panel, charge controller, and deep-cycle battery were installed next to the monitoring manhole to provide power to run the sampling pump.

3.4. Monitoring Filter Outflows

Stone collected the first set of grab samples and measured water quality parameters on March 18, 2022, and continued monitoring filter inflows and outflows approximately weekly through December 15, 2022. Samples were collected following rainstorms when possible. Filter inflow samples were collected by dipping sample bottles at the openings of intake pipes IN1 and IN2. Filter outflow samples were collected using a peristaltic pump to withdraw water from the sampling port on each filter outlet pipe (Figure 4). Samples were processed in the field for TP and TDP analysis. Sample processing procedures are described in the QAPP (Appendix A).

The temperature, pH, and specific conductivity of the filter inflows and outflows were measured during each sampling visit using an Oakton pH/Con 10 meter, according to the Study Specific Procedure 19-020-1.0, included with the QAPP (Appendix A). The pH/Con 10 meter requires daily calibration of the pH and conductivity sensors.

The Zenner ZSU ultrasonic flowmeters transmitted cumulative flow totals to remote displays located outside the monitoring manhole. We determined that these flowmeters could not be



Figure 4. Sample collection

interfaced with common types of data loggers. Therefore, we read the cumulative flow total from the flowmeter remote display and entered this value in a custom Survey123 field form. We recorded cumulative flow totals immediately before and after sample collection. The elapsed time between readings was typically 45–60 minutes. To calculate the flow rate during sample collection, the difference between the successive flow total readings was calculated and divided by the elapsed time.

Water samples were transported to VAEL by courier within the stated holding times for each analyte. Samples were tracked using a Chain of Custody form that accompanied water samples delivered to VAEL. Once the water samples were accepted by VAEL, they were subject to the lab's internal tracking system.

3.5. Water Sample Analysis

Water samples were analyzed by the standard methods of VAEL. These methods and relevant data quality objectives, assessment procedures, and reporting limits are described in VAEL's Quality Systems Manual, Revision 25, dated April 13, 2020. The methods of analysis are included with the QAPP (Appendix A) and are summarized in Table 3. Approved analytical data are included in Appendix D.

Table 3. Water analysis methods

Analyte	Lab	Method
TP	VAEL	VAEL SOP SM 4500-P H
TDP	VAEL	VAEL SOP SM 4500-P H

3.6. Challenges Encountered

There was a recurrent problem in the TDP analysis of F_{AA} outflow samples. Fifteen (nearly half) of the F_{AA} TDP concentration results were substantially higher than expected, more than 130% of the TP value for the corresponding sample. In four cases the TDP value was more than ten times the TP value. These values included TDP concentrations as high as 851 $\mu\text{g/L}$. These anomalous values were censored as invalid in the dataset (Appendix D). Valid duplicate sample data were available on two dates. After reviewing analytical data for several rounds of sampling in March-April 2022, Stone tried to remedy the problem by changing the brand of membrane filter used to process TDP samples in the field. After anomalous F_{AA} TDP results were seen in later rounds of samples, we concluded the membrane filters were not the problem. As it became apparent that the problem was confined to F_{AA} , we began to suspect an unknown analytical interference. We contacted VAEL repeatedly to inquire about potential analytical interference in the F_{AA} samples, possibly due to aluminum (considering the composition of the media). The VAEL nutrient chemistry analytical leader was not aware of any potential interference in the TDP analytical method from aluminum.

Specifications for the 2-inch Zenner ZSU ultrasonic flowmeter state an accurate flow measurement range of 0.25–230 GPM (0.95–871 L/min) and a “start-up” flow rate (essentially a low-flow cutoff) of 0.12 GPM (0.45 L/min). While measurement of 0.95 L/min is considered quite sensitive, actual flow rates were below 0.95 L/min during many sampling events. As expected, as the pond level dropped all the filters stopped flowing between July and October 2022 for periods lasting days or weeks. On other sampling events, certain filter outlets were visibly trickling, while the flowmeters recorded zero flow or values in the 0.12–0.25 GPM (0.45–0.95 L/min) range, which was also expected. This occurred on one event at F_{SBS} , eight events at F_{DWTR} , and eleven events at F_{ZVI} . In each case, the F_{AA} outlet was still flowing at >0.95 L/min. When the filter outlets were visibly flowing, the outflows were sampled per our standard procedures regardless of the flowmeter readings. However, we used regression relationships between F_{AA} and F_{SBS} , F_{DWTR} , and F_{ZVI} flow rates to estimate very low flow rates at F_{SBS} , F_{DWTR} , and F_{ZVI} . These estimated low flow rates were used in subsequent P loading calculations.

4. Quality Assurance Tasks Completed

The project data-quality objective was to collect, provide, maintain, analyze, display, and document valid water quantity and quality data. Field quality assurance measures included adherence to the QAPP, Version 1, approved July 16, 2020 (Appendix A).

The analytical laboratory for the water samples was VAEL. VAEL is accredited by New Hampshire under the National Environmental Laboratory Accreditation Program (NELAP) for the specified water quality parameters. Sample analyses by VAEL were conducted according to the laboratory's established procedures, which are described in VAEL's Quality Systems Manual, Revision 25, dated April 13, 2020. This manual identifies the analytical methods and relevant data quality objectives, assessment procedures, and reporting limits applied.

Field quality control sampling consisted of duplicate grab samples submitted to VAEL for TP and TDP analysis. Field duplicates were collected of TP and TDP samples on a rotating basis among the filter inflows and outflows. Data from field duplicates were accepted if the Relative Percent Difference (RPD) was less than or equal to 20%; in such cases, the mean of the field duplicates was used to represent data from the sample involved.

Sampling QC excursions were evaluated by the Project Manager. Field duplicate sample results were used to assess the entire sampling process, including environmental variability; therefore, the arbitrary rejection of results based on predetermined limits was not practical. The professional judgment of the Project Manager was relied upon in evaluating results.

Reasons for rejecting certain sample results were determination that the results were not representative due to an adverse field condition or an evident analytical error. Data and observations describing such conditions and errors are distilled in comments included in Appendix D in the "VAEL Remarks" and "Comments" fields. Censored data are summarized in Table 4.

Table 4. Summary of invalid TP and TDP data

Sites	Dates	Censored data	Comment
IN1, IN2	12/15/2022	TP concentrations and loads invalid	Technician broke through ice, muddying pond
F _{AA}	Multiple	TDP concentration and load data invalid: 3/18, 4/14, 4/21, 5/5, 5/13, 5/17 (valid dupe), 6/16, 6/23, 7/1, 7/7, 8/13, 9/29 (valid dupe), 10/5, 11/28, and 12/8; TP concentration and load data invalid on 12/8	Suspected analytical Interference
F _{SBS}	3/18/2022	TP concentration and load invalid	
F _{SBS}	5/5/2022	TDP concentration and load invalid (valid dupe)	
F _{SBS}	12/8/2022	TDP concentration and load data invalid (valid dupe); TP concentration and load data invalid (valid dupe);	VAEL code: TDP matrix interference
F _{DWTR}	8/13/2022	TDP concentration and load invalid (valid dupe)	VAEL estimated TP

5. Phosphorus Filter Results

Between March 18 and December 15, 2022, water samples were collected approximately weekly at intakes IN1 and IN2 and the outflows from F_{AA} through F_{ZVI} . Temperature, pH, and specific conductivity measurements made at the filter intakes and outflows during each sampling visit are tabulated in Appendix D. Appendix D also includes the approved TP and TDP concentration data from VAEL and filter outflow rates recorded during sample collection, calculated as the elapsed outflow volume divided by the elapsed time.

Since inflow rates to the filters were not measured directly, we assumed that filter inflow rates were equivalent to the monitored outflow rates. The filters were lined in durable plastic; therefore, minimal groundwater exchange should occur. The sum of the flow rates from F_{AA} and F_{SBS} should equal the actual (unmeasured) flow rate at the IN1 intake, and the sum of the flow rates from F_{DWTR} and F_{ZVI} should equal the actual flow rate at the IN2 intake.

Instantaneous TP and TDP loading rates in filter outflow were calculated from TP and TDP concentrations and corresponding outflow rates. These data are included in Appendix D. P loading rates in filter inflow were calculated as the inflow P concentration multiplied by the outflow rate. P loading rates are expressed as P mass (mg) per unit time (hr). The hour duration of the P loading rates reflects the 45–60-minute sampling period over which the “instantaneous” flow rates were calculated.

There was a maximum of 30 paired events for each filter. As discussed in Sections 3.6 and 5.1.3, there were numerous events with invalid TDP results at F_{AA} , which reduced the sample size to 19 for the F_{AA} TDP concentration and loading analyses. Additionally, three sampling events were excluded from all statistical analysis because of exceedingly low outflow rates (events on June 16 and October 5, 2022) or freezing conditions at the intakes (December 15, 2022). Exclusion of these outlier events improved the fit of regression analyses presented in Sections 5.2.1, 5.2.2, and 5.2.3.

5.1. Summary of Water Quality, Flow Rate, and P Loading Data at Inflows and Outflows

Tables 5 through 12 present summary statistics for water quality parameters measured in the field (temperature, pH, and specific conductivity) and flow rates and TP and TDP concentrations and instantaneous loads at filter inflows and outflows at the time of sample collection.

The inflow water quality parameters are identical for F_{AA} and F_{SBS} (Tables 5 and 6) because these measurements were taken at the inlet of the common intake pipe (IN1). The same is true for the water quality parameters measured at intake IN2 to F_{DWTR} and F_{ZVI} (Tables 7 and 8). The inflow P concentrations for F_{DWTR} and F_{ZVI} are likewise identical. The inflow concentrations of TP and TDP are nearly identical for F_{AA} and F_{SBS} (Tables 5 and 6), the exception being a single

sample that was included in the F_{SBS} inflow dataset ($n = 30$) and excluded in the F_{AA} inflow dataset ($n = 29$). The flow rates differ substantially among the four filters and the inflow P loading rates differ accordingly (Tables 5-8). In contrast, the outflow P concentrations and P loading rates (Tables 9-12) reflect both differences in their flow rates and the actions of the filters.

Table 5. Descriptive statistics for F_{AA} inflows

	Temp. (C)	pH (su)	Sp. Cond. ($\mu\text{g/L}$)	TP Conc. ($\mu\text{g/L}$)	TDP Conc. ($\mu\text{g/L}$)	Flow rate (L/min)	TP Load (mg/hr)	TDP Load (mg/hr)
Count	30	30	30	29	29	30	29	29
Min	2.5	6.4	272	25.7	14.8	9.05	32.8	17.8
25th%	7.1	6.9	641	43.0	29.4	17.0	61.1	39.8
Median	15.5	7.1	907	99.6	65.4	22.5	136	80.9
75th%	20.1	7.3	1171	144	86.2	33.9	164	111
Max	26.2	7.5	1849	432	158	153	953	665
Mean	14.2	7.1	939	115	63.4	34.8	228	133
St. Dev.	7.22	0.25	399	87.6	39.6	34.0	273	166

Table 6. Descriptive statistics for F_{SBS} inflows

	Temp. (C)	pH (su)	Sp. Cond. ($\mu\text{g/L}$)	TP Conc. ($\mu\text{g/L}$)	TDP Conc. ($\mu\text{g/L}$)	Flow rate (L/min)	TP Load (mg/hr)	TDP Load (mg/hr)
Count	30	30	30	30	30	30	30	30
Min	2.5	6.4	272	25.7	14.8	3.50	15.1	10.9
25th%	7.1	6.9	641	43.6	29.6	10.1	58.7	28.4
Median	15.5	7.1	907	96.1	64.1	16.5	86.4	53.4
75th%	20.1	7.3	1171	143	83.7	34.3	174	100
Max	26.2	7.5	1849	432	158	162	972	678
Mean	14.2	7.1	939	114	62.9	30.7	184	113
St. Dev.	7.22	0.25	399	86.2	39.0	36.0	234	166

Table 7. Descriptive statistics for F_{DWTR} inflows

	Temp. (C)	pH (su)	Sp. Cond. ($\mu\text{g/L}$)	TP Conc. ($\mu\text{g/L}$)	TDP Conc. ($\mu\text{g/L}$)	Flow rate (L/min)	TP Load (mg/hr)	TDP Load (mg/hr)
Count	30	30	30	30	30	30	30	30
Min	2.6	6.4	263	25.9	16.4	0.66	2.32	1.19
25th%	7.0	6.9	688	51.3	27.0	2.95	14.4	7.54
Median	15.2	7.1	899	90.9	57.2	5.33	28.7	17.6
75th%	19.7	7.3	1144	140	77.1	17.2	66.0	39.6
Max	25.9	7.6	1805	276	113	130	709	540

Mean	14.3	7.1	943	101	56.9	18.0	96.0	66.0
St. Dev.	7.15	0.27	380	60.1	31.3	29.4	174	134

Table 8. Descriptive statistics for F_{ZVI} inflows

	Temp. (C)	pH (su)	Sp. Cond. ($\mu\text{g/L}$)	TP Conc. ($\mu\text{g/L}$)	TDP Conc. ($\mu\text{g/L}$)	Flow rate (L/min)	TP Load (mg/hr)	TDP Load (mg/hr)
Count	30	30	30	30	30	30	30	30
Min	2.6	6.4	263	25.9	16.4	0.48	1.01	0.52
25th%	7.0	6.9	688	51.3	27.0	1.40	8.19	4.04
Median	15.2	7.1	899	90.9	57.2	2.84	12.5	8.18
75th%	19.7	7.3	1144	140	77.1	8.30	43.2	27.8
Max	25.9	7.6	1805	276	113	62.7	376	275
Mean	14.3	7.1	943	101	56.9	9.86	56.1	37.3
St. Dev.	7.15	0.27	380	60.1	31.3	16.1	103	73.6

Table 9. Descriptive statistics for F_{AA} outflows

	Temp. (C)	pH (su)	Sp. Cond. ($\mu\text{g/L}$)	TP Conc. ($\mu\text{g/L}$)	TDP Conc. ($\mu\text{g/L}$)	Flow rate (L/min)	TP Load (mg/hr)	TDP Load (mg/hr)
Count	30	30	29	29	19	30	29	19
Min	2.9	5.6	289	21.0	14.4	9.05	29.6	19.8
25th%	6.9	6.1	702	37.2	34.9	17.0	53.5	42.2
Median	15.6	6.3	934	65.1	48.0	22.5	95.2	83.1
75th%	19.3	6.7	1164	95.4	73.1	33.9	152	134
Max	25.5	7.2	1842	267	217	153	730	668
Mean	14.2	6.4	958	87.2	63.6	34.8	165	159
St. Dev.	6.99	0.43	382	70.1	48.9	34.0	190	191

Table 10. Descriptive statistics for F_{SBS} outflows

	Temp. (C)	pH (su)	Sp. Cond. ($\mu\text{g/L}$)	TP Conc. ($\mu\text{g/L}$)	TDP Conc. ($\mu\text{g/L}$)	Flow rate (L/min)	TP Load (mg/hr)	TDP Load (mg/hr)
Count	30	30	30	30	29	30	30	29
Min	2.5	6.0	279	22.3	14.8	3.50	16.4	9.61
25th%	7.0	6.5	744	40.3	26.2	10.1	56.5	40.1
Median	15.7	6.6	927	76.3	53.3	16.5	92.8	74.5
75th%	19.6	6.8	1199	134	100	34.3	192	101
Max	25.5	7.3	1881	649	243	162	850	632
Mean	14.1	6.6	982	125	73.4	30.7	174	108
St. Dev.	7.12	0.30	393	132	63.4	36.0	207	147

Table 11. Descriptive statistics for F_{DWTR} outflows

	Temp. (C)	pH (su)	Sp. Cond. ($\mu\text{g/L}$)	TP Conc. ($\mu\text{g/L}$)	TDP Conc. ($\mu\text{g/L}$)	Flow rate (L/min)	TP Load (mg/hr)	TDP Load (mg/hr)
Count	30	30	30	30	30	30	30	30
Min	2.6	6.2	281	22.8	14.8	0.66	1.68	1.18
25th%	7.5	6.6	741	36.1	28.0	2.95	8.06	6.47
Median	15.5	6.8	902	56.5	37.1	5.33	18.2	13.3
75th%	19.1	6.9	1125	65.4	46.4	17.2	42.4	34.7
Max	25.4	7.2	1840	150	66.7	130	549	481
Mean	14.2	6.8	967	59.5	39.0	18.0	72.8	50.4
St. Dev.	6.96	0.26	384	29.9	14.0	29.4	142	106

Table 12. Descriptive statistics for F_{ZVI} outflows

	Temp. (C)	pH (su)	Sp. Cond. ($\mu\text{g/L}$)	TP Conc. ($\mu\text{g/L}$)	TDP Conc. ($\mu\text{g/L}$)	Flow rate (L/min)	TP Load (mg/hr)	TDP Load (mg/hr)
Count	30	30	30	30	30	30	30	30
Min	3.2	6.5	288	25.7	12.5	0.48	0.77	0.55
25th%	8.1	6.7	664	31.6	20.5	1.40	2.70	1.78
Median	15.6	6.9	841	41.7	25.2	2.84	7.31	3.26
75th%	19.6	7.1	1124	58.3	31.2	8.30	22.7	12.9
Max	25.2	7.4	1819	142	58.5	62.7	239	161
Mean	14.3	6.9	909	48.8	27.4	9.86	35.5	20.2
St. Dev.	6.93	0.24	373	25.4	10.1	16.1	67.5	39.6

Data for the four filters are compared in Sections 5.1.1 through 5.1.4. The boxplots in Figure 5 through Figure 11 illustrate the distributions of the water quality data collected at the filter inflow and outflow monitoring locations. The top and bottom of the vertical box indicate the 75th and 25th percentiles, respectively, of the data distribution for the category, defining the interquartile range. The horizontal line across each box indicates the median (50th percentile) of the data distribution. The top and bottom vertical lines (“whiskers”) for each box define the [3rd quartile + 1.5 x interquartile range] and the [1st quartile – 1.5 x interquartile range], respectively. Points beyond the whiskers represent outliers.

5.1.1. Water quality parameters

Temperature data (Figure 5, Tables 5-8) reveal tremendous seasonal variability at the filter inflows, from 2.5 to 26.2°C. Maximum temperatures (~25°C) were measured in late July and early August. On December 15, 2022, filter inflow samples were collected after breaking through the pond ice. While there was high variability in temperature over the monitoring period, there

was little difference among the filter outflows on any given date. In each filter, outflow temperatures were not significantly different ($p < 0.10$) from inflow temperatures.

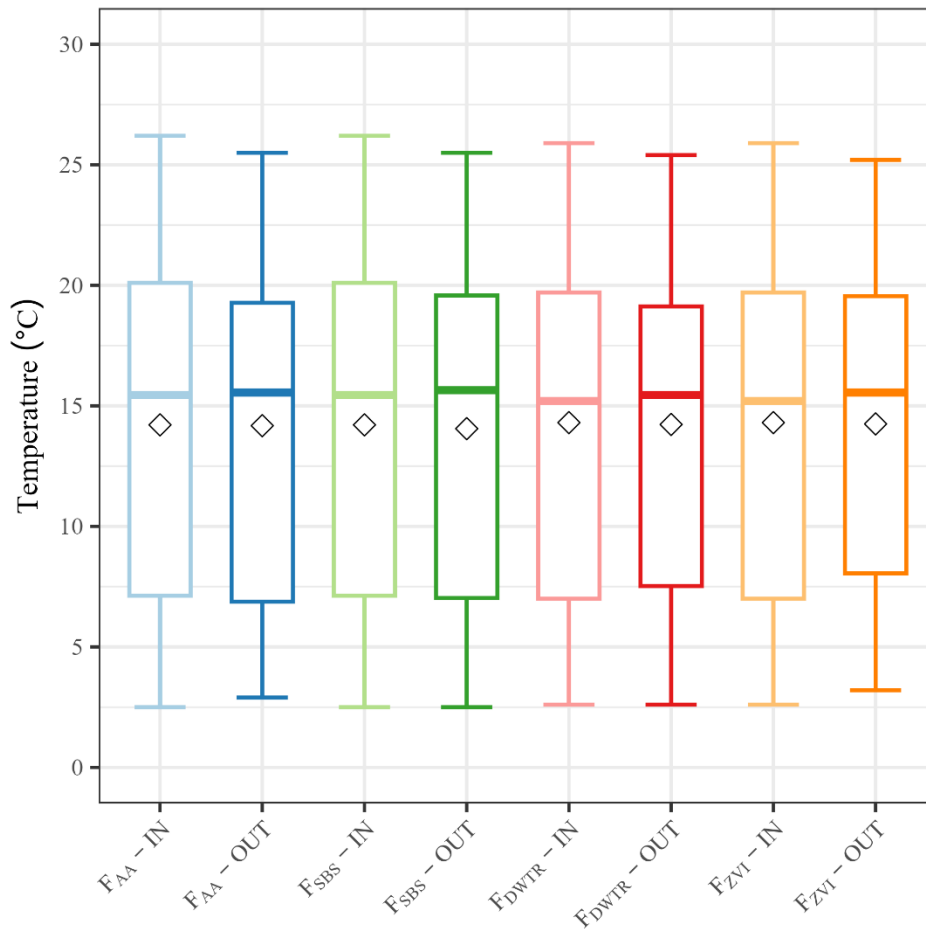


Figure 5. Distributions of temperature at filter inflows and outflows

The pH data (Figure 6, Tables 5-8) reveal low variability at the filter inflows over the monitoring period, from 6.4 to 7.6 (median = 7.1). However, the pH of the filter outflows was significantly lower ($p < 0.10$) than the inflows at all four filters. In particular, the pH of the F_{AA} outflow was often unacceptably low relative to the Vermont Water Quality Standards (VTANR 2022). The median pH value (6.3) was lowest in F_{AA} outflow, followed by F_{SBS} (6.6) and F_{DWTR} (6.8) outflows. The median pH of the F_{ZVI} outflow (6.9) was only slightly lower than in the inflow (7.1).

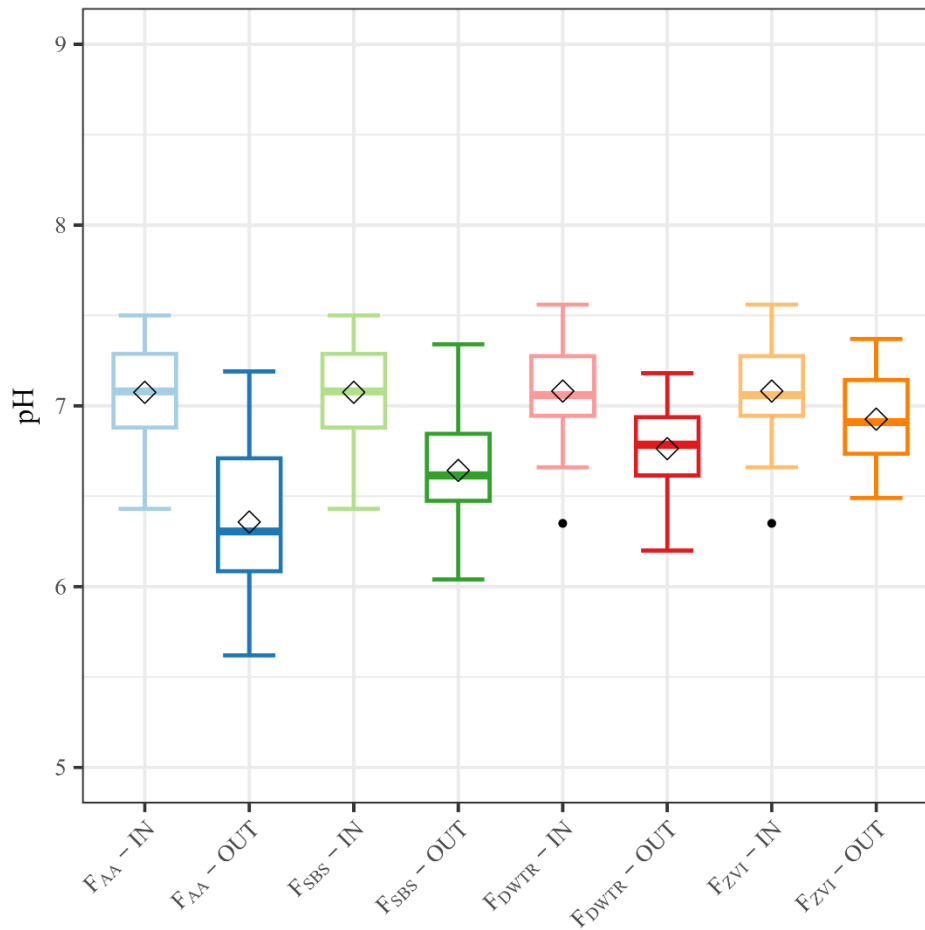


Figure 6. Distributions of pH at filter inflows and outflows

As with temperature, the specific conductivity data (Figure 7, Tables 5-8) reveal great variability at the filter inflows over the monitoring period. The median specific conductivity of the filter inflows was ~900 $\mu\text{S}/\text{cm}$. Maximum specific conductivities (1805 $\mu\text{S}/\text{cm}$ at IN1 and 1849 $\mu\text{S}/\text{cm}$ at IN2) were measured on March 24, 2022, presumably associated with runoff of deicing salt. Minimum specific conductivities (272 $\mu\text{S}/\text{cm}$ at IN1 and 263 $\mu\text{S}/\text{cm}$ at IN2) were measured on September 14, 2002. While there was high variability in specific conductivity over the monitoring period, there was little difference among the filter outflows on any given date. In each filter, specific conductivity was not significantly different ($p < 0.10$) between inflows and outflows.

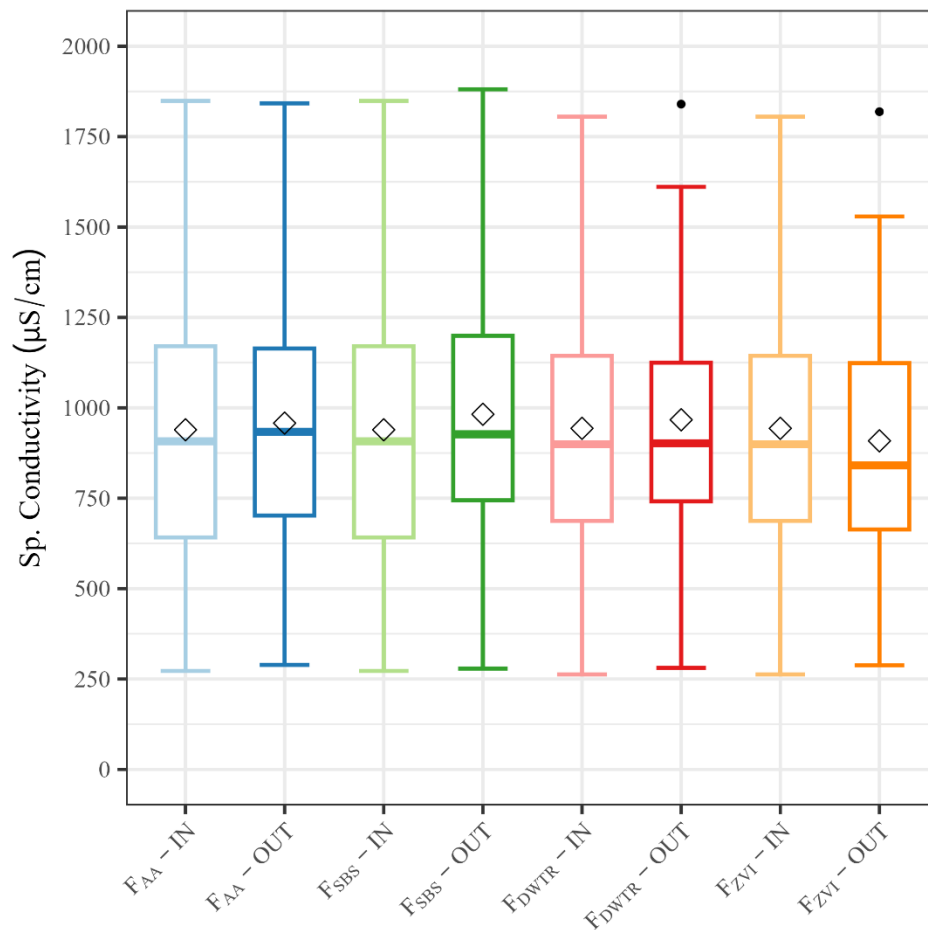


Figure 7. Distributions of specific conductivity at filter inflows and outflows

5.1.2. Flow rates

As described in Section 3.4, “instantaneous” flow rates were calculated at the time of sampling by calculating the elapsed flow volume from cumulative flow total readings immediately before and after sampling and dividing the elapsed volume by the elapsed time to derive a flow rate.

Instantaneous outflow rates and cumulative volumes varied substantially among the four filters (Tables 5-12). Unfortunately, flow rates and cumulative volumes corresponded with the position of the filters (generally $F_{AA} > F_{SBS} > F_{DWTR} > F_{ZVI}$), presumably due to slight differences in hydraulic gradient. F_{AA} , closest to the pond outlet, had the highest median instantaneous flow rate (22.5 L/min). Over the monitoring period, F_{AA} passed the greatest cumulative volume (8,586,748 L). F_{ZVI} , furthest from the pond outlet, had the lowest median instantaneous flow rate (2.8 L/min) and cumulative volume (2,033,748 L). At the median flow rates, the residence time of water in these filters ranged from 69 minutes (F_A) to 557 minutes. (F_{ZVI}). At the maximum flow rates recorded, 153 L/min from F_{AA} and 162 L/min for F_{SBS} , the residence time of water in these filters was approximately 10 minutes. This is shorter than the minimum residence time of

15-20 minutes we were intending to achieve, which may have decreased the effectiveness of F_{AA} and F_{SBS} at the highest flow rates.

5.1.3. TP and TDP concentrations

Intake IN1 had TP concentrations ranging from 25.7–432 $\mu\text{g/L}$, and a median concentration of 99.6 $\mu\text{g/L}$ (Table 5). IN2 had TP concentrations ranging from 25.9–276 $\mu\text{g/L}$, and a median concentration of 90.9 $\mu\text{g/L}$ (Table 7). TDP concentrations in inflow were somewhat lower: 14.8–158 $\mu\text{g/L}$ (median = 65.4 $\mu\text{g/L}$) for IN1 (Table 5) and 16.4–113 $\mu\text{g/L}$ (median = 57.2 $\mu\text{g/L}$) for IN2 (Table 7).

Only paired inflow/outflow data are plotted in the TP and TDP concentration boxplots presented in Figures 8 and 9. Figure 8 illustrates that outflows from all four filters had lower TP concentrations than corresponding inflows. For each filter, the minimum, 25th percentile, median, and 75th percentile TP concentrations were lower in outflows than in inflows. However, these differences were only statistically significant ($p < 0.10$) for F_{DWTR} and F_{ZVI} . F_{ZVI} outflows had a median TP concentration of 41.7 $\mu\text{g/L}$ (Table 12), approximately 54% lower than the inflow (90.9 $\mu\text{g/L}$). F_{DWTR} outflows had a median concentration of 56.5 $\mu\text{g/L}$ (Table 11), approximately 38% lower than the inflow.

A similar pattern is apparent in the TDP concentration data. Figure 9 illustrates that outflow from all four filters typically had lower TDP concentrations than corresponding inflows, with some exceptions. Median TDP concentrations were lower in outflows from all four filters. However, these differences were only statistically significant ($p < 0.10$) for F_{DWTR} and F_{ZVI} . F_{ZVI} outflows had a very low median TDP concentration of 25.2 $\mu\text{g/L}$ (Table 12), approximately 56% lower than the inflow (57.2 $\mu\text{g/L}$). F_{DWTR} outflows had a median TDP concentration of 37.1 $\mu\text{g/L}$ (Table 11), approximately 35% lower than the inflow.

Exceptions occurred in outflows from F_{AA} and F_{SBS} , which had maximum TDP concentrations that substantially exceeded corresponding inflow concentrations. Regarding F_{AA} , we believe this result reflects the recurrent problem with TDP analysis of F_{AA} outflow samples (see Section 3.6). Despite censoring 15 F_{AA} TDP results for suspected analytical interference, among the remaining data there may be additional TDP concentration values affected by the suspected analytical problem, possibly including the maximum value (243 $\mu\text{g/L}$). Regarding F_{SBS} , the maximum TDP outflow concentration may have exceeded the inflow concentration due to release of TDP from the filter media under summer low flow conditions, when this result occurred.

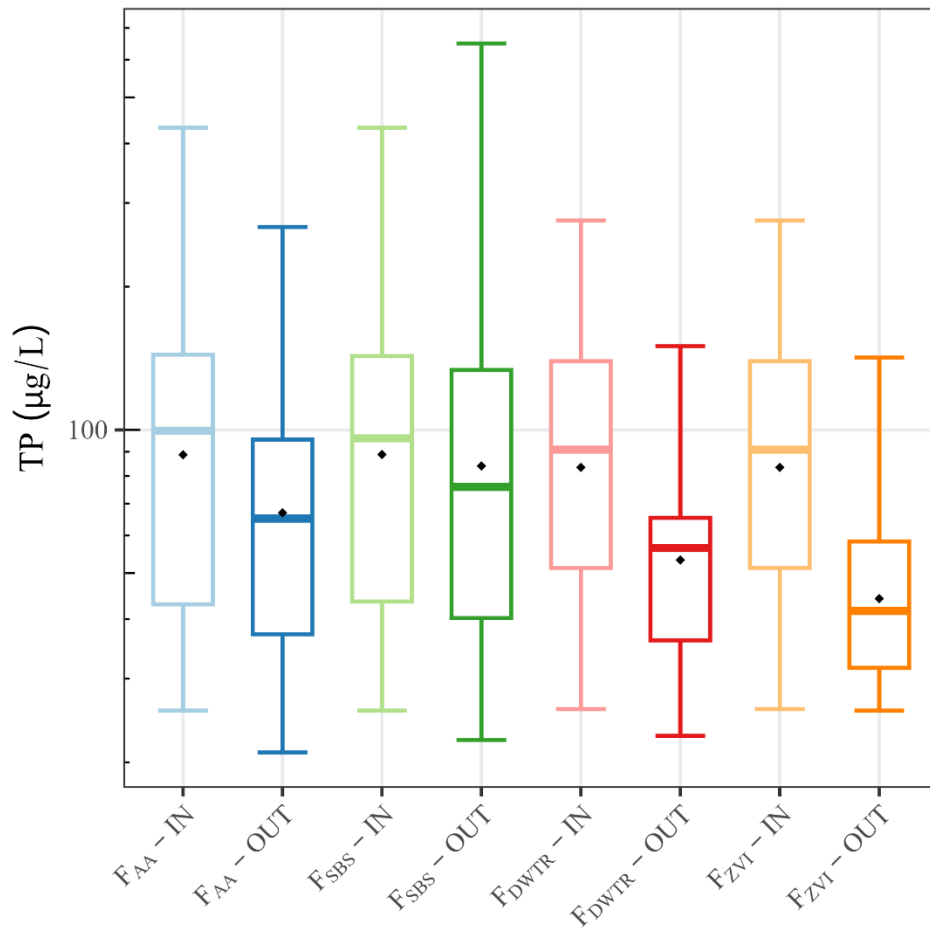


Figure 8. Distributions of TP concentrations at filter inflows and outflows

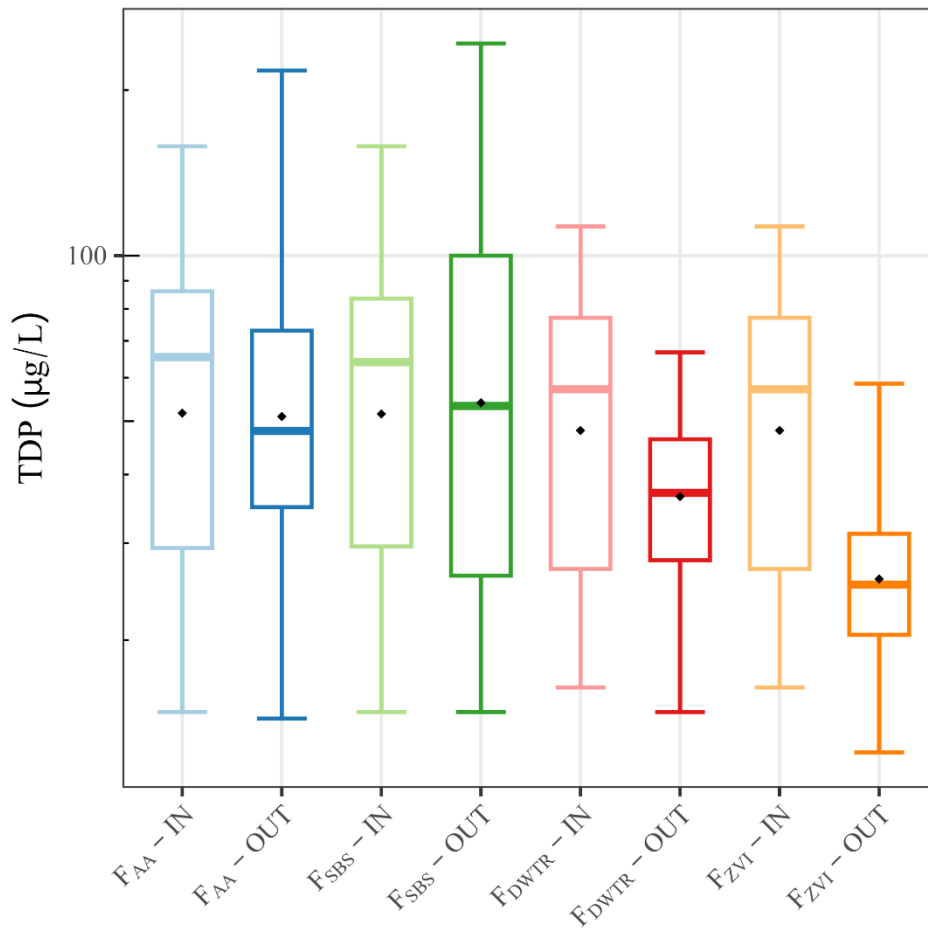


Figure 9. Distributions of TDP concentrations at filter inflows and outflows

5.1.4. TP and TDP loading

Figures 10 and 11 present distributions of instantaneous TP and TDP loading rates in filter inflows and outflows. Only paired inflow/outflow loading data are used in these boxplots. TP loading at the filter inflows ranged from 32.8–953 mg/hr (median = 136 mg/hr) for F_{AA} , 15.1–972 mg/hr (median = 86.4 mg/hr) for F_{SBS} , 2.32–709 mg/hr (median = 28.7 mg/hr) for F_{DWTR} , and 1.01–376 mg/hr (median = 12.5 mg/hr) for F_{ZVI} (Tables 5-8). The equivalent inflow TDP loading rates were: 17.8–665 mg/hr (median = 80.9 mg/hr) for F_{AA} , 10.9–678 mg/hr (median = 53.4 mg/hr) for F_{SBS} , 1.19–540 mg/hr (median = 17.6 mg/hr) for F_{DWTR} , and 0.52–275 mg/hr (median = 8.18 mg/hr) for F_{ZVI} .

At F_{AA} , F_{DWTR} , and F_{ZVI} , TP loads (Figure 10) and TDP loads (Figure 11) appear lower in the outflow than in the inflow. At F_{SBS} (SBS only), there is little discernible difference in TP loads between the inflow and outflow. The TDP loads follow a similar pattern, with the exception that there is little discernible difference between inflow and outflow TDP loads at F_{AA} and a suggested increase between inflow and outflow TDP loads at F_{SBS} .

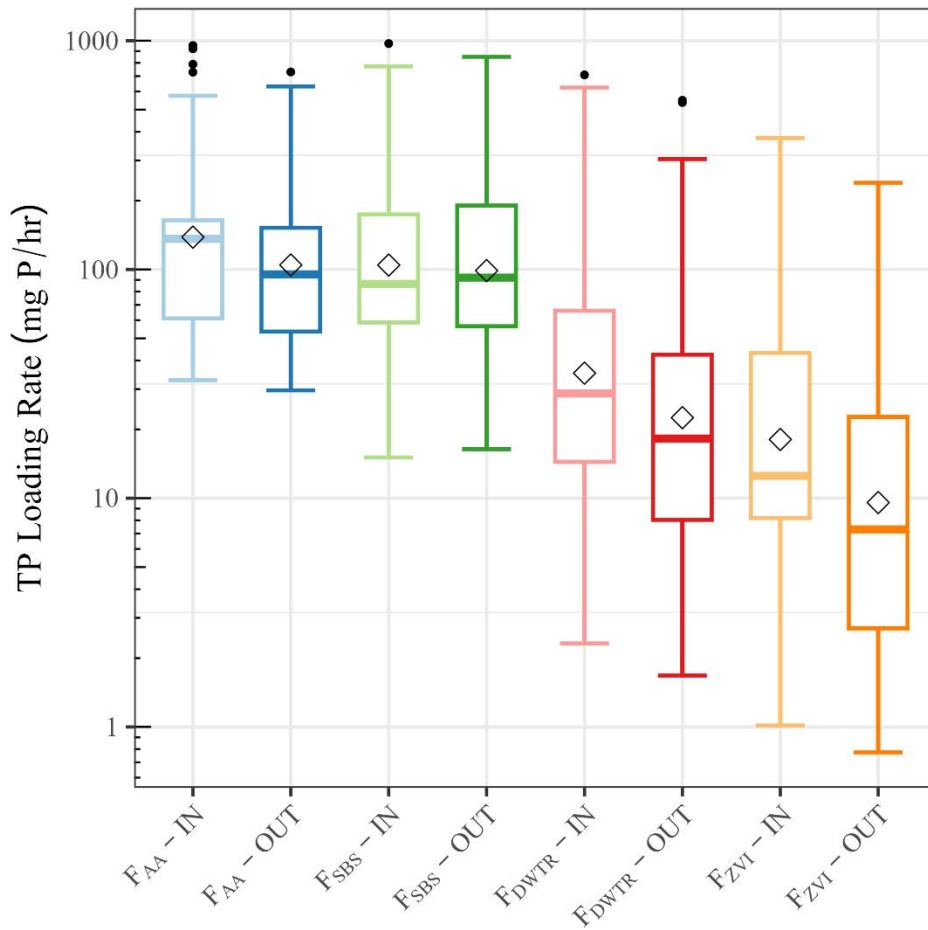


Figure 10. Distributions of TP loading rates at filter inflows and outflows

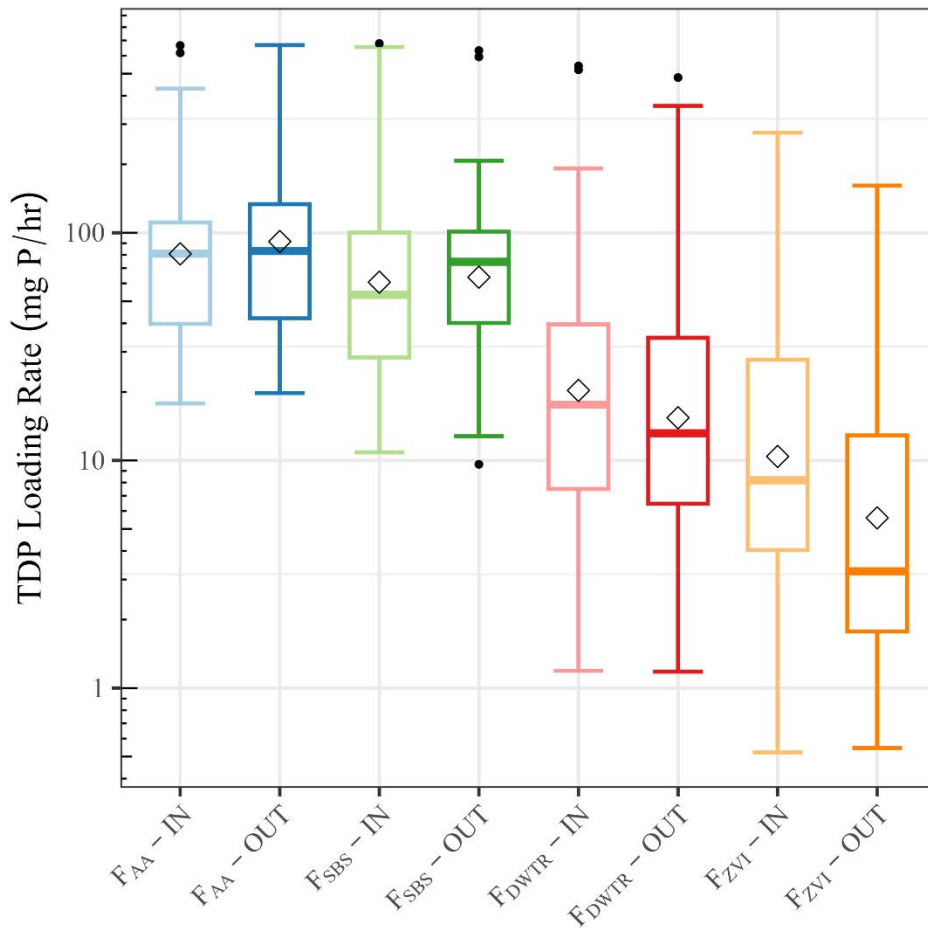


Figure 11. Distributions of TDP loading rates at filter inflows and outflows

5.1.5. TP and TDP concentration timeseries

Figures 12 and 13 show timeseries plots of TP and TDP concentrations. The timeseries plots reveal seasonal differences in TP and TDP concentrations at the filter intakes. TP and TDP concentrations at the intakes were higher in summer than in spring or fall. Fluctuations in the inflow TP and TDP concentrations are generally reflected in fluctuations in filter outflow concentrations. Notwithstanding high outliers in the F_{AA} and F_{SBS} TP concentration timeseries (Figure 12), the seasonal pattern is reasonably clear.

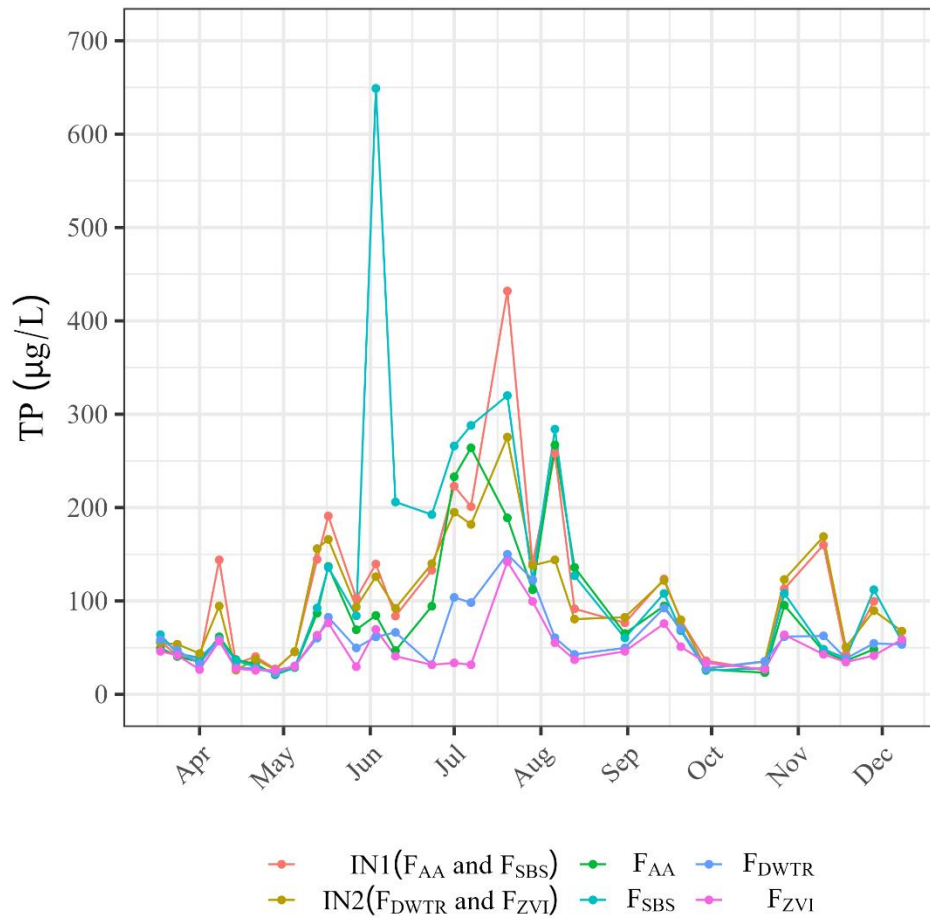


Figure 12. TP concentration timeseries at filter inflows and outflows

Figure 13 reveals an unexpected pattern in the TDP concentrations in the F_{SBS} outflow. Between June 3 and August 31, 2022, the TDP concentration in the F_{SBS} outflow exceeded the inflow TDP concentration—often substantially—on 9 of 11 sampling dates. These data suggest the Swanton black shale media contributed P during this low flow period, which is clearly not a good result.

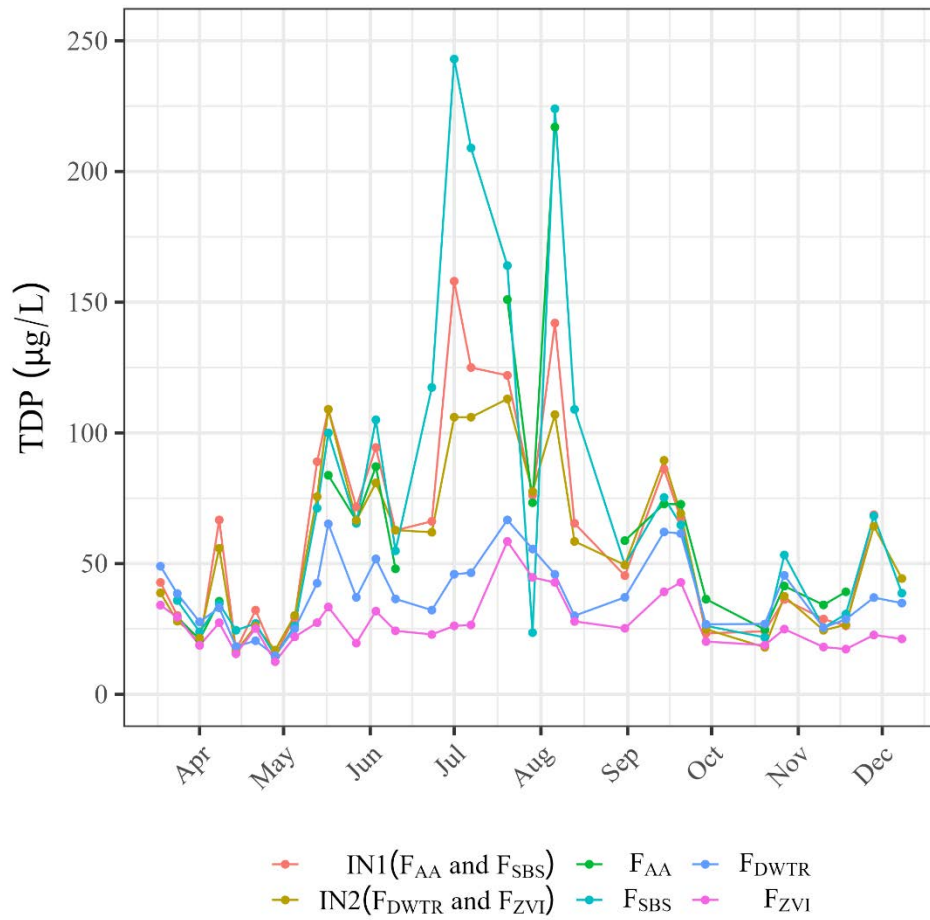


Figure 13. TDP concentration timeseries at filter inflows and outflows

Overall, inflow TP and TDP concentrations are higher in mid-summer than in spring and fall. TP and TDP concentration boxplots in Figure 14 suggest this pattern holds for 25th, 50th, and 75th percentile TP and TDP concentration values at both filter intakes.

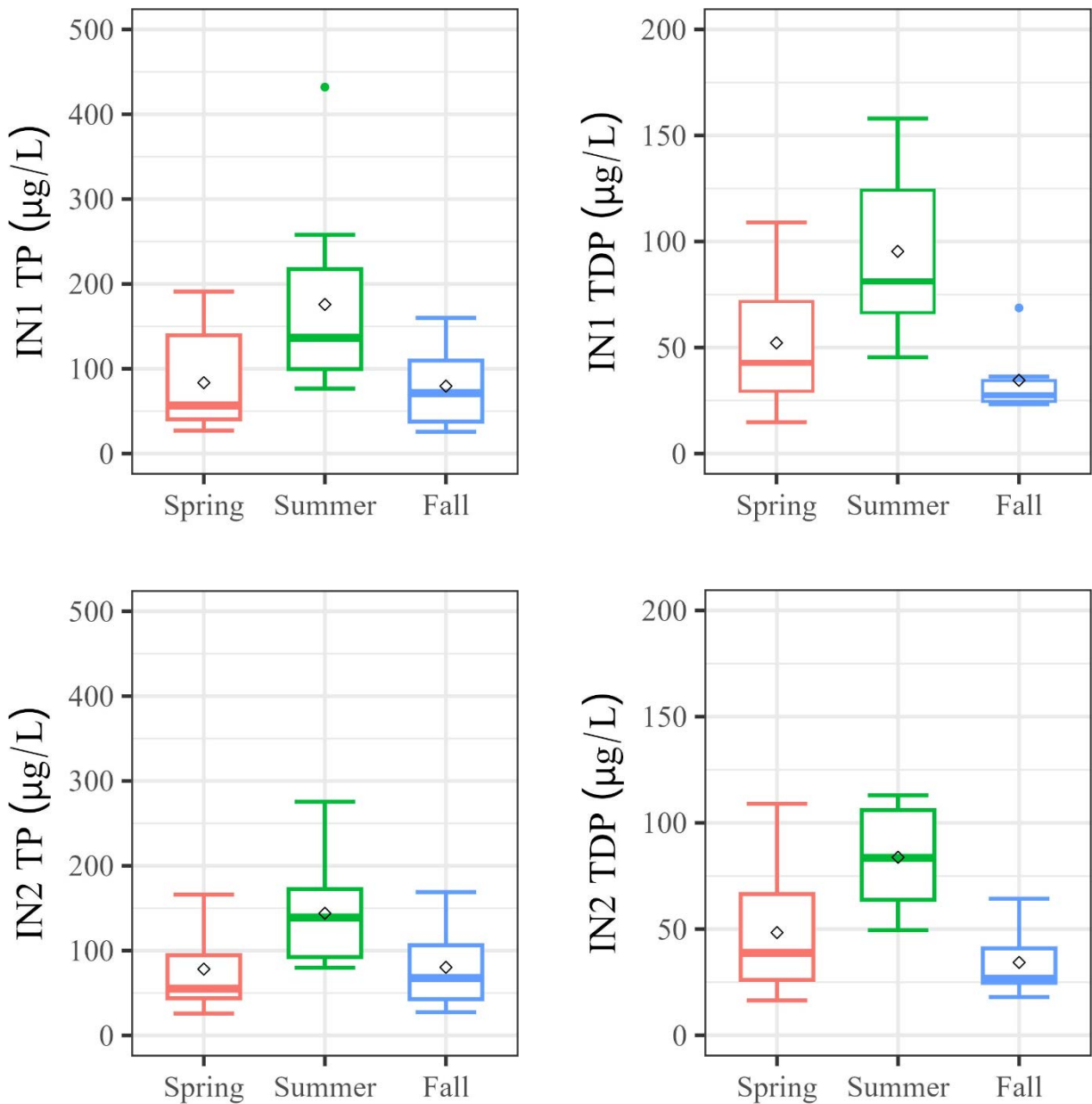


Figure 14. TP and TDP concentration distributions at filter intakes by season

5.2. P Filter Performance

Statistical analysis of the filter inflow and outflow data was conducted according to EPA guidance for monitoring and evaluating nonpoint source management practices (Dressing et al. 2016) using an “input/output” experimental design. Filter performance was quantified using trimmed datasets with non-paired data removed.

TP and TDP concentration and instantaneous loading data were tested for normality using the Shapiro-Wilks method in R. The concentration and loading data do not follow normal distributions. Therefore, non-parametric Wilcoxon rank sum tests were used to assess the inflow and outflow data distributions for significant differences. The results of two-sided Wilcoxon rank sum tests are provided in Table 13. Significant differences ($p < 0.10$) were found for F_{DWTR} in TP and TDP concentrations, but not loads. For F_{ZVI} , significant differences were found in both TP and TDP concentrations and loads. No significant differences were found for F_{AA} and F_{SBS} in TP or TDP concentrations or loads.

Table 13. P-values from Wilcoxon rank sum tests between filter inflows and outflows¹

Filter	TP (µg/L)	TDP (µg/L)	TP Load (mg/hr)	TDP Load (mg/hr)
F_{AA}	0.14	0.94	0.19	0.74
F_{SBS}	0.67	0.97	0.92	0.62
F_{DWTR}	0.0081	0.052	0.19	0.58
F_{ZVI}	0.0002	0.00017	0.072	0.068

1. Statistically significant reductions in bold face

The reduction efficiencies of the P filters were calculated using the percent reductions in P concentrations as well as regression of outflow vs. inflow P concentrations and loads, after Dressing et al. (2016). Overall efficiency was determined for each filter by calculating the average P concentrations for inflows and outflows and using these values to calculate the percent change in concentration. Table 14 presents the overall efficiency estimates. Because average values are compared, these estimates do not consider paired data.

Table 14. Percent reductions in P concentrations between filter inflows and outflows

Filter	Concentration Reduction ¹ (%)	
	TP	TDP
F_{AA}	23.9	-0.2
F_{SBS}	-9.7	-16.7
F_{DWTR}	40.9	31.5
F_{ZVI}	51.5	51.9

1. Statistically significant reductions in bold face

The P concentration reductions presented in Table 14 provide a reasonable basis for comparing the filters. F_{AA} and F_{SBS} performed surprisingly poorly. Any apparent TP and TDP concentration reductions through the filters were non-significant. F_{DWTR} reduced concentrations of TP by 40.9% and TDP by 31.5%. F_{ZVI} reduced TP and TDP concentrations by 51.5% and 51.9%.

5.2.1. Simple linear regressions on inflow/outflow P concentrations

Figures 15 through 18 present simple linear regressions of filter outflow P concentrations versus inflow P concentrations. The trendlines are forced through the origin. 95% confidence intervals calculated about the regression lines are also shown. The significance of the relationships was assessed using the Spearman's rho test. All relations between outflow and inflow P concentrations were significant at $p < 0.05$.

The slopes of the TP and TDP concentration regression lines are substantially less than 1 for both F_{DWTR} (Figure 17) and F_{ZVI} (Figure 18), suggesting reduction of P through the filters. Conversely, the slopes of the TP and TDP concentration regression lines for both F_{AA} (Figure 15) and F_{SBS} (Figure 16) approach one, suggesting little P removal.

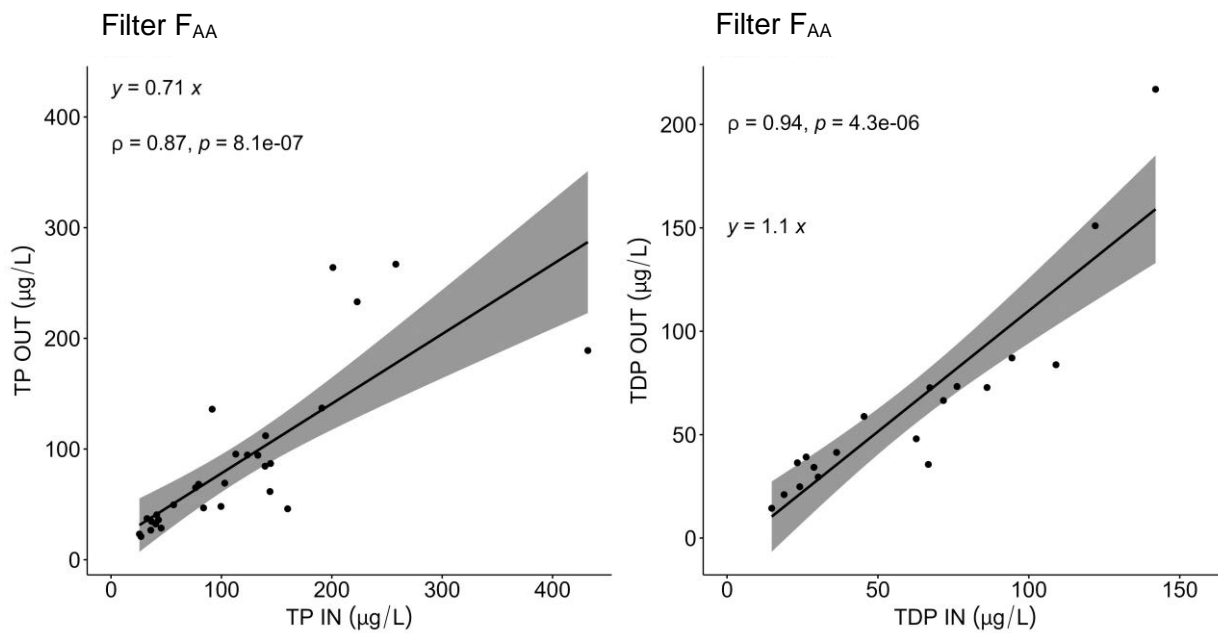


Figure 15. Regression of F_{AA} inflow/outflow TP (left) and TDP (right) concentrations

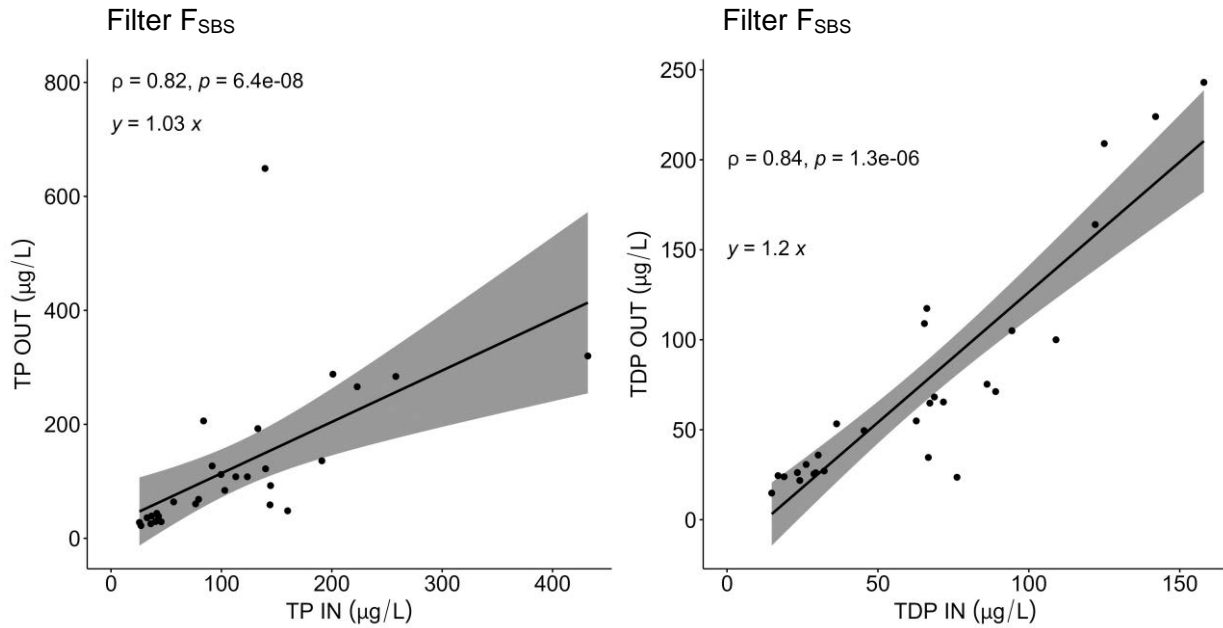


Figure 16. Regression of F_{SBS} inflow/outflow TP (left) and TDP (right) concentrations

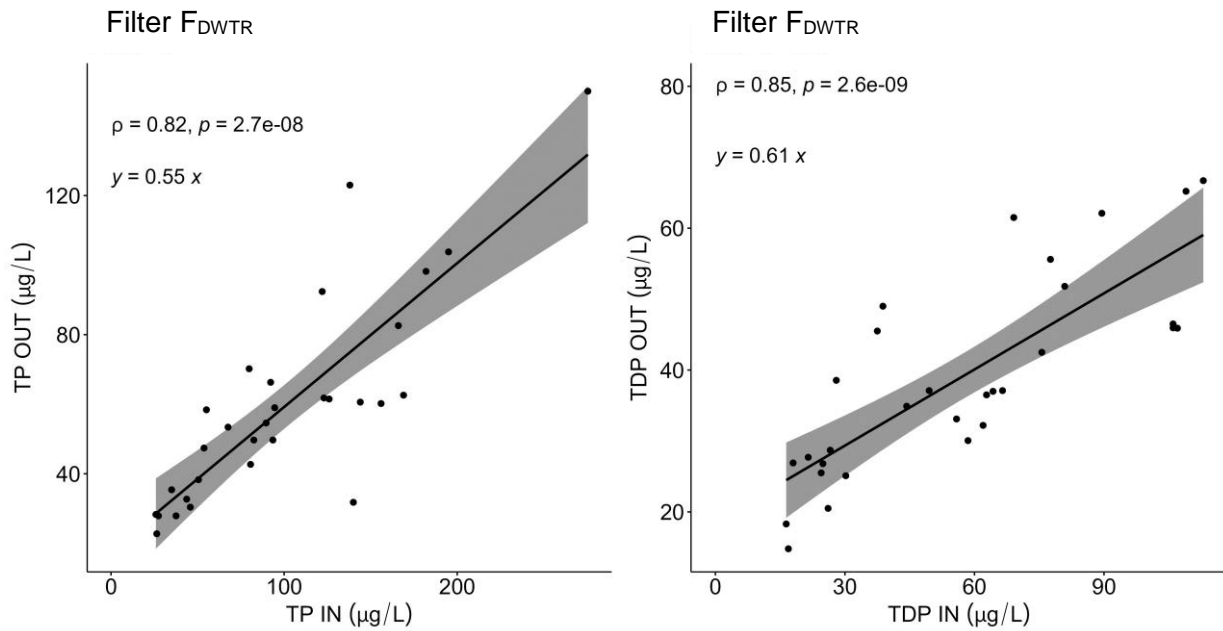


Figure 17. Regression of F_{DWTR} inflow/outflow TP (left) and TDP (right) concentrations

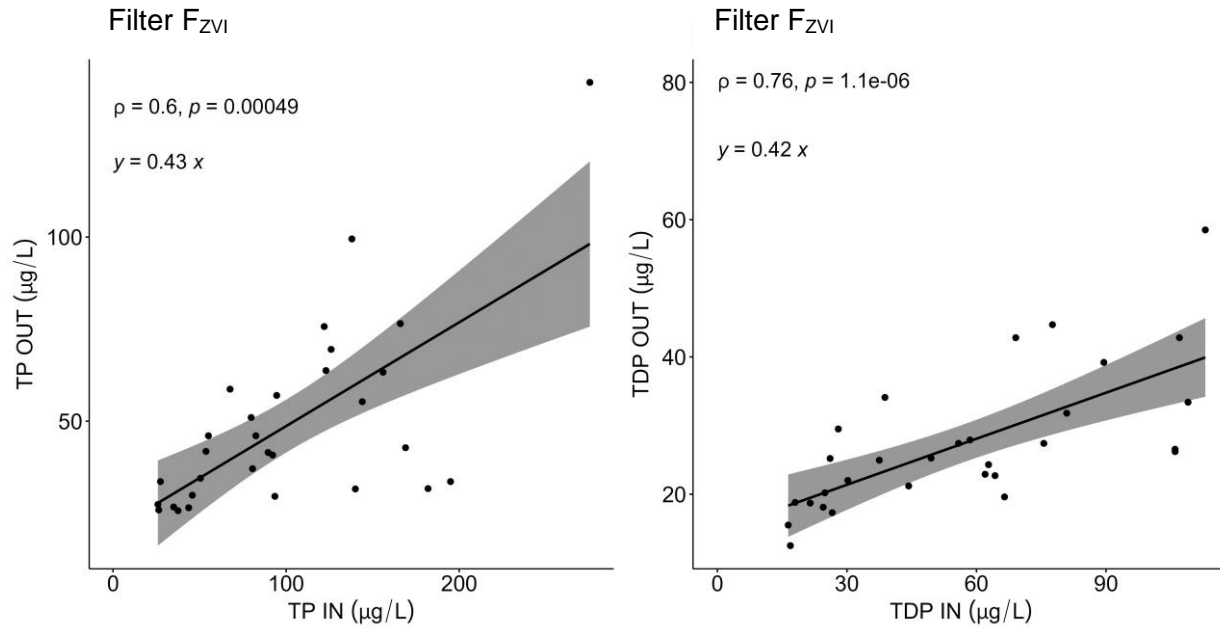


Figure 18. Regression of F_{ZVI} inflow/outflow TP (left) and TDP (right) concentrations

5.2.2. Simple linear regressions on inflow/outflow P loads

Similar patterns are apparent in simple linear regressions of filter outflow P loads versus inflow P loads (Figures 19-22). Again, the trendlines are forced through the origin. 95% confidence intervals calculated about the regression lines are also shown. The significance of the relationships was assessed using the Spearman's rho test. All relations between outflow and inflow P loads were significant at $p < 0.05$.

The slopes of the F_{ZVI} TP (0.65) and TDP (0.53) load regression lines (Figure 22) are lowest among the filters. These provide further evidence that P loads were reduced through F_{ZVI} . The slope (0.68) of the F_{AA} TP load regression line (Figure 19) also suggests some P load reduction, although the difference was not significant using the Wilcoxon rank sum test (Table 13). In contrast, the slopes of the F_{AA} TDP (0.95), F_{SBS} TP (0.85), and F_{SBS} TDP (0.86) load regression lines are close to 1, suggesting little or no consistent P load reduction (Figures 19 and 20). While the TP and TDP load regressions at F_{DWTR} were highly significant ($p < 2.2e-16$), the slopes of the regression lines (TP = 0.80 and TDP = 0.78) suggest only marginal load reduction (Figure 21).

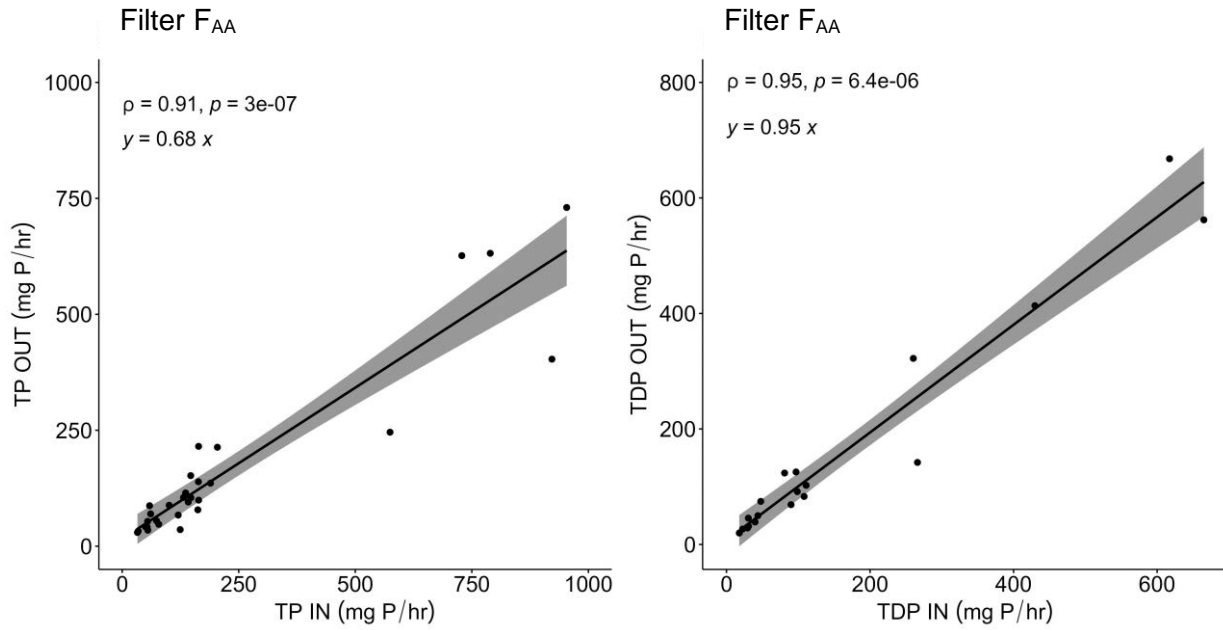


Figure 19. Regression of F_{AA} inflow/outflow TP (left) and TDP (right) loading

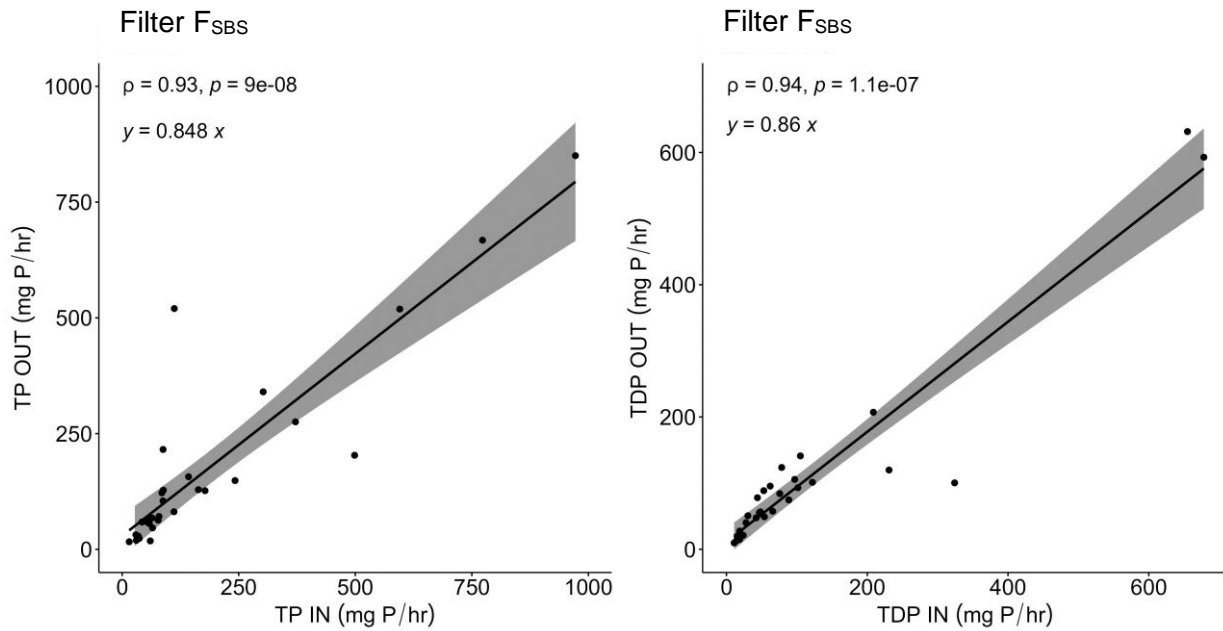


Figure 20. Regression of F_{SBS} inflow/outflow TP (left) and TDP (right) loading

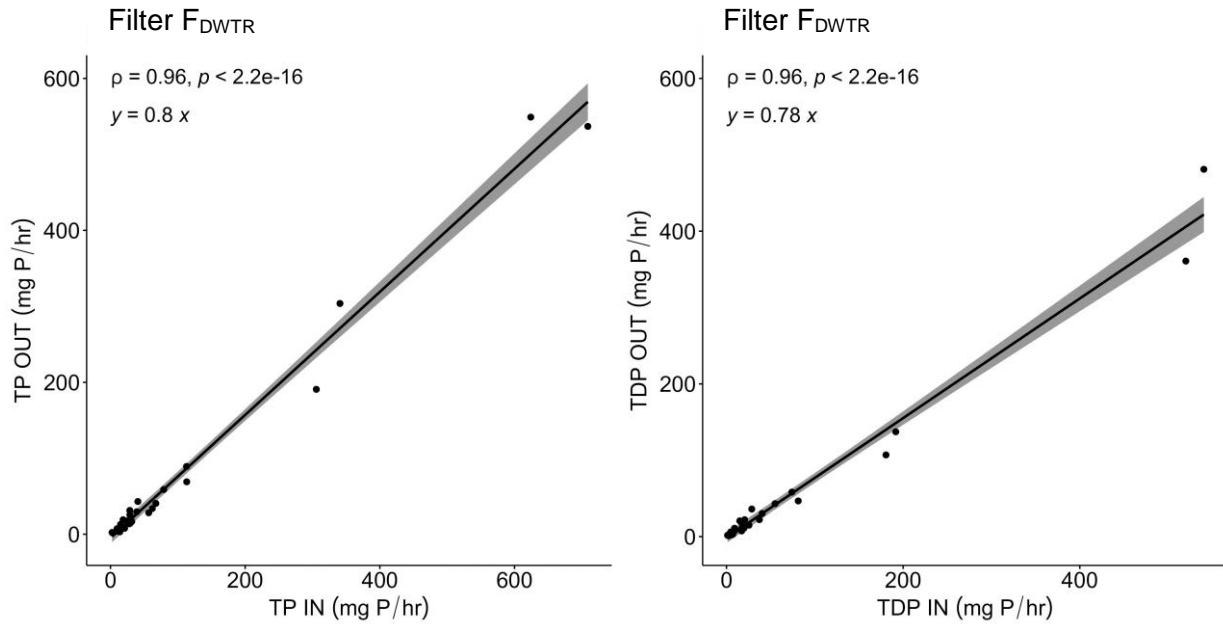


Figure 21. Regression of F_{DWTR} inflow/outflow TP (left) and TDP (right) loading

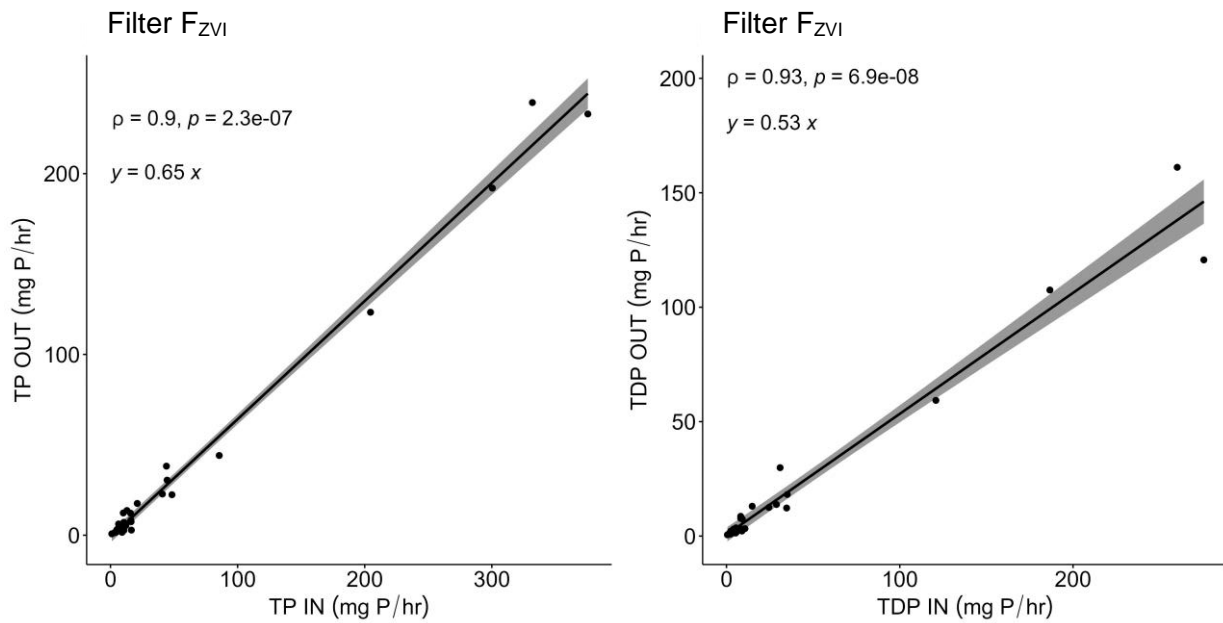


Figure 22. Regression of F_{ZVI} inflow/outflow TP (left) and TDP (right) loading

The slopes of regression equations between inflow and outflow concentrations and loads provide alternate estimates of filter performance (Table 15). The significance of the differences between inflow and outflow P concentration and load distributions was previously assessed using Wilcoxon rank sum tests (Table 13).

Table 15. P concentration and load reduction estimates from linear regression equations

Filter	Concentration Reduction Estimates from Regression Line Slopes ¹ (%)		Load Reduction Estimates from Regression Line Slopes ¹ (%)	
	TP (µg/L)	TDP (µg/L)	TP Load (mg/hr)	TDP Load (mg/hr)
F _{AA}	29	-10	32	5
F _{SBS}	-3	-20	15	14
F _{DWTR}	45	39	20	22
F _{ZVI}	57	58	35	47

1. Statistically significant reductions in bold face

Among the statistically significant results in Table 15, F_{DWTR} reduced TP concentrations by 45% and TDP concentrations by 39%. F_{ZVI} was substantially more effective, reducing TP and TDP concentrations by 57% and 58%, and TP and TDP loads by 35% and 47%. Any effects of F_{AA} and F_{SBS} on TP and TDP concentrations and loads were not significant.

5.2.3. Simple linear regressions of percent reduction on inflow P concentration

The efficiency with which a filter may remove a given constituent often varies as a function of the constituent's inflow concentration. Establishing the concentration range over which a filter is effective is critical in selecting appropriate locations to install P filters. In Figures 23-26, P reduction efficiencies (%) among paired inflow/outflow P concentrations are regressed on inflow P concentrations. The regressions for F_{DWTR} (Figure 25) and F_{ZVI} (Figure 26) are significant at p<0.05. Regressions for F_{AA} (Figure 23) and F_{SBS} (Figure 24) are not significant. As is often the case, there is a great deal of scatter in the P reduction efficiency data at low inflow P concentrations. This was true for both TP and TDP.

Using the regression equations indicated in Figures 23-26, we calculated predicted P reductions at F_{DWTR} and F_{ZVI} for representative inflow P concentrations. Toward the low end (~25th percentile) of the inflow TP concentration range (48 µg/L), F_{DWTR} and F_{ZVI} reduced TP concentrations by 19% and 26%, respectively. Toward the low end (~25th percentile) of the inflow TDP concentration range (30 µg/L), F_{DWTR} and F_{ZVI} reduced TDP concentrations by 47% and 25%. At 95 µg/L TP and 60 µg/L TDP—median inflow concentrations—F_{DWTR} and F_{ZVI} were moderately effective, reducing TP concentrations by 31% and 40% and TDP concentrations by 69% and 44%, respectively. Finally, at 140 µg/L TP and 80 µg/L TDP—75th percentile inflow concentrations—F_{DWTR} and F_{ZVI} reduced TP concentrations by 41% and 53% and TDP concentrations by 84% and 56%, respectively. While TP and TDP reductions are also suggested at F_{AA}, these differences were not statistically significant. P reductions were not demonstrated nor suggested at F_{SBS}.

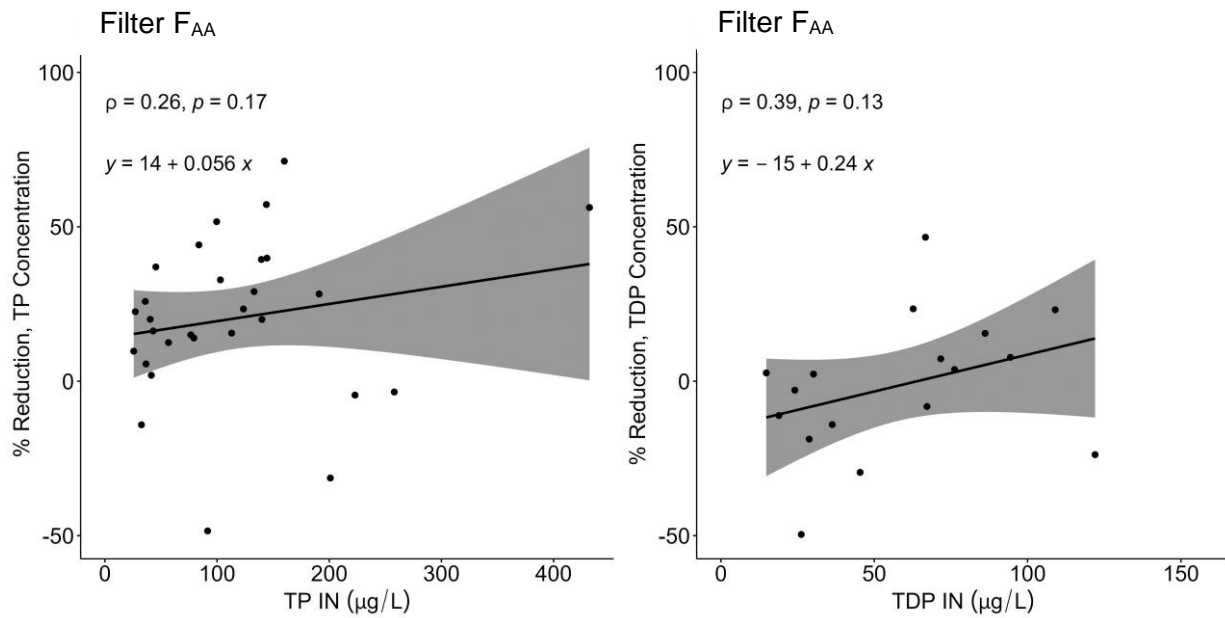


Figure 23. Percent reduction of inflow TP (left) and TDP (right) concentrations at F_{AA}

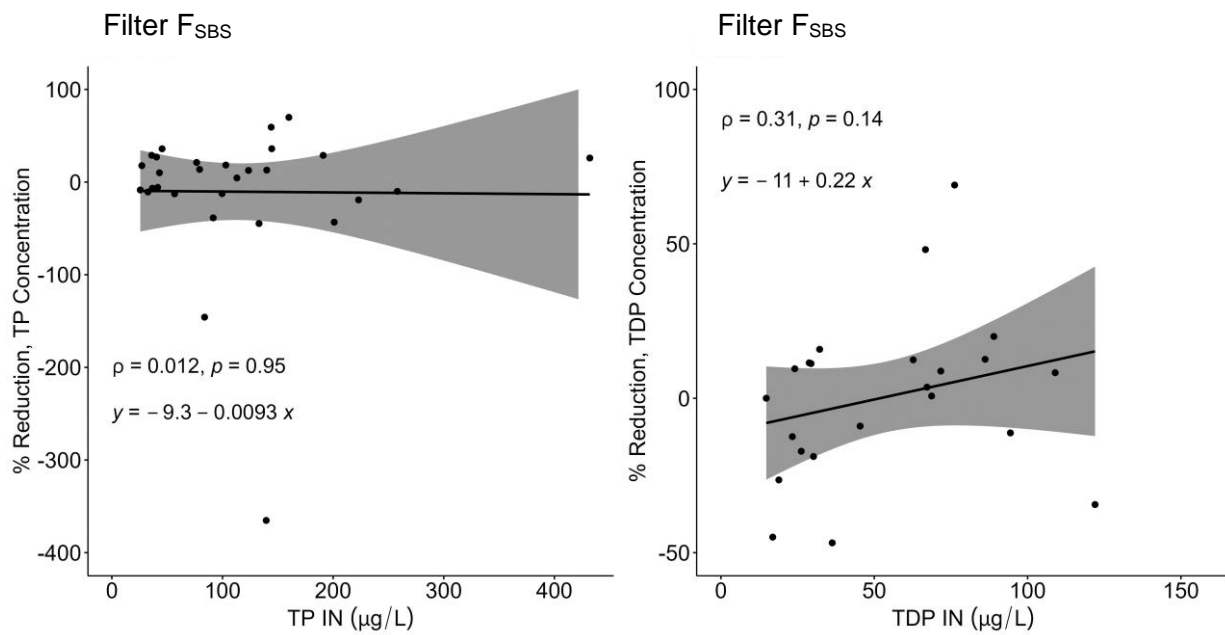


Figure 24. Percent reduction of inflow TP (left) and TDP (right) concentrations at F_{SBS}

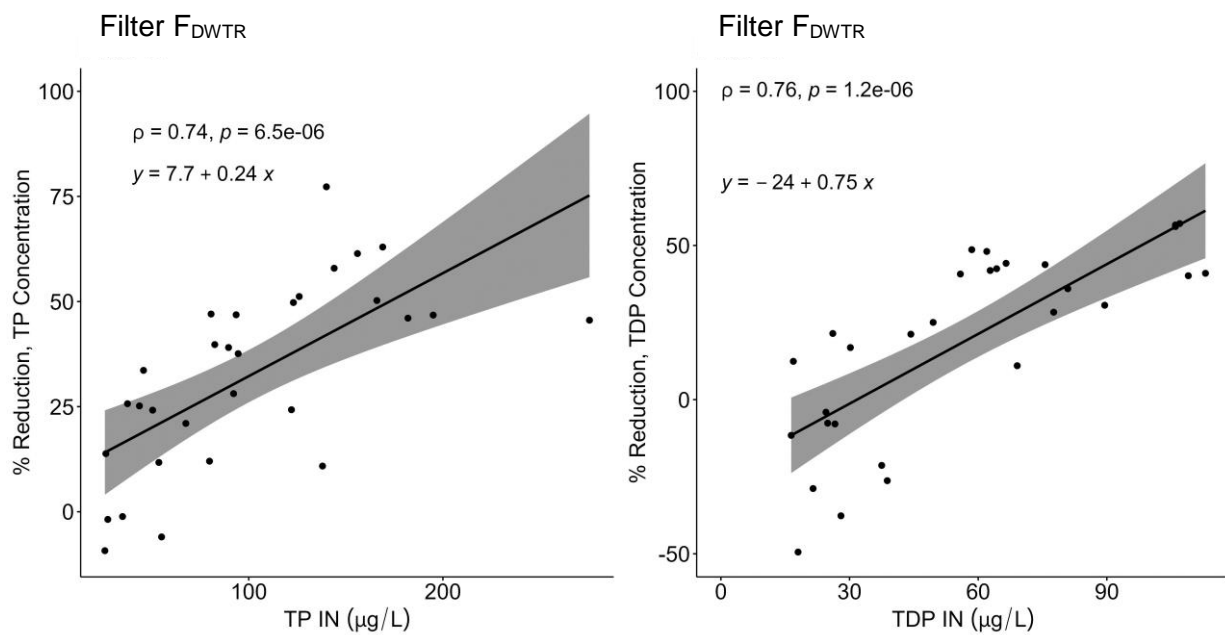


Figure 25. Percent reduction of inflow TP (left) and TDP (right) concentrations at F_{DWTR}

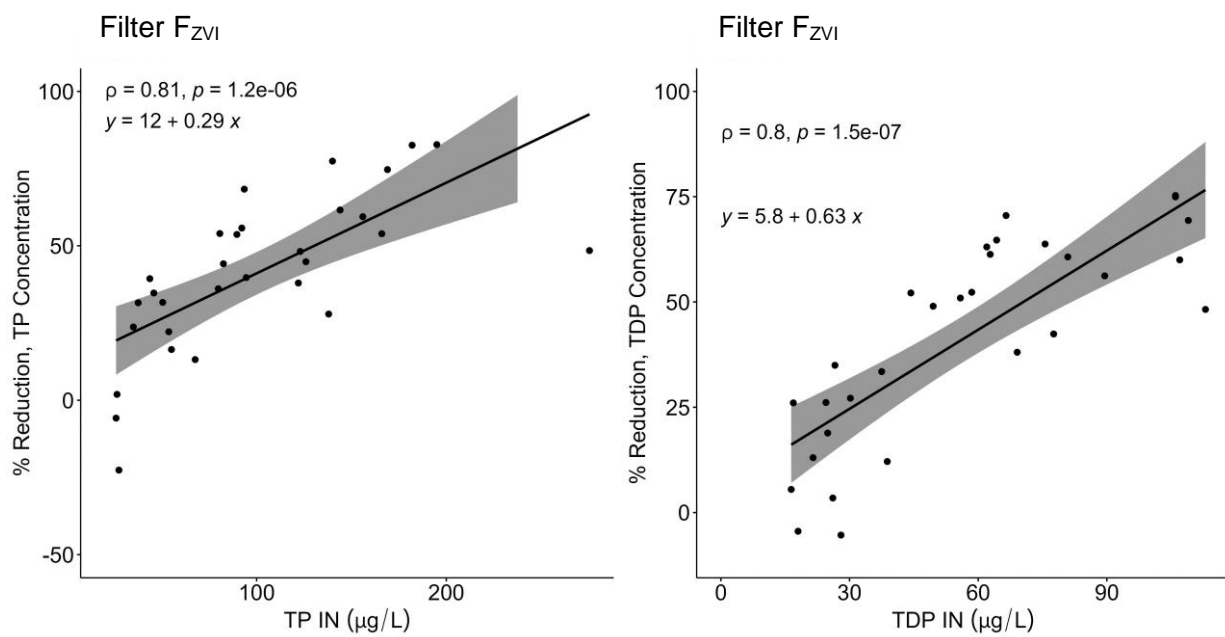


Figure 26. Percent reduction of inflow TP (left) and TDP (right) concentrations at F_{ZVI}

5.2.4. Filter performance relative to flow rate

To examine the effect of flow rate on performance of the P filters, the data were stratified into low, moderate, and high flow strata and reanalyzed. In Figure 27, percent reductions in TP concentration between inflows and outflows were regressed on inflow TP concentrations, in strata according to flow rate.

Regressions at F_{AA} and F_{SBS} were not significant at $p < 0.10$, with the exception of the mid-flow strata at F_{AA} . At F_{DWTR} regressions were significant in the mid- and high-flow strata, but not in the low-flow strata. At F_{ZVI} regressions were significant in all three flow strata. The relationships in all three flow strata appear reasonably consistent, indicating that P reduction was achieved at F_{ZVI} across the range of observed inflow rates. These regressions illustrate a strong dependence of P reduction efficiency on inflow TP concentration. The F_{DWTR} and F_{ZVI} regression lines were similar in all three flow strata, which suggests that retention times in the filters were adequate to reduce P at moderate and high flow rates (i.e., the filter flow rates were not excessive).

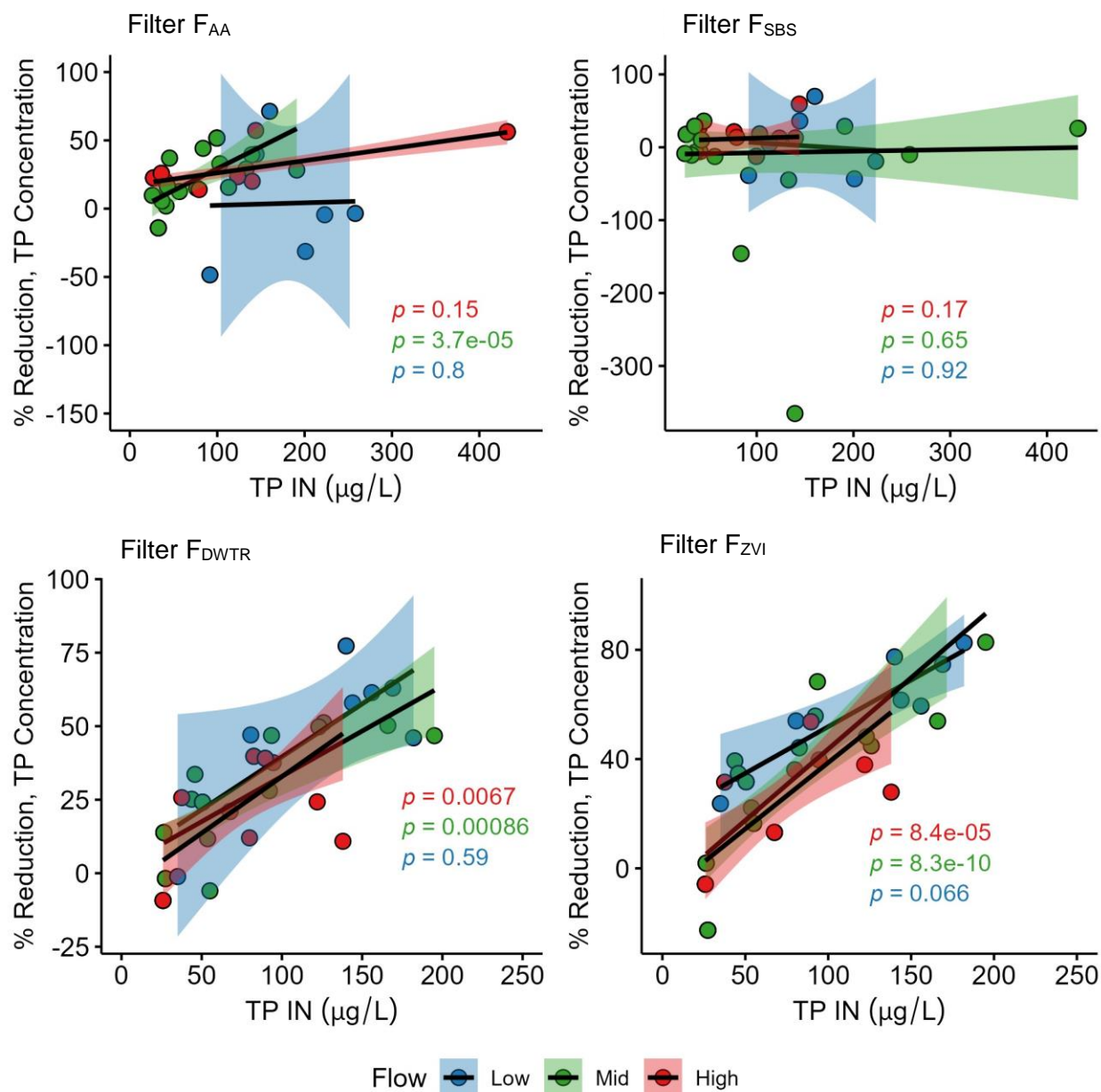


Figure 27. Percent reduction of inflow TP concentrations grouped by flow strata

Figure 28 shows percent reductions in TDP concentration between inflows and outflows regressed on inflow TDP concentrations stratified by flow rate. At both F_{DWTR} and F_{ZVI} , all regressions were significant at $p < 0.10$. These regressions illustrate a strong dependence of P reduction efficiency on inflow TDP concentration, which holds in all three flow strata. Results for F_{AA} and F_{SBS} are less clear. A significant regression was only found in the mid-flow strata at F_{AA} . We are not convinced the F_{AA} and F_{SBS} results are particularly meaningful, except as further demonstration of the lack of consistent P reduction by these filters.

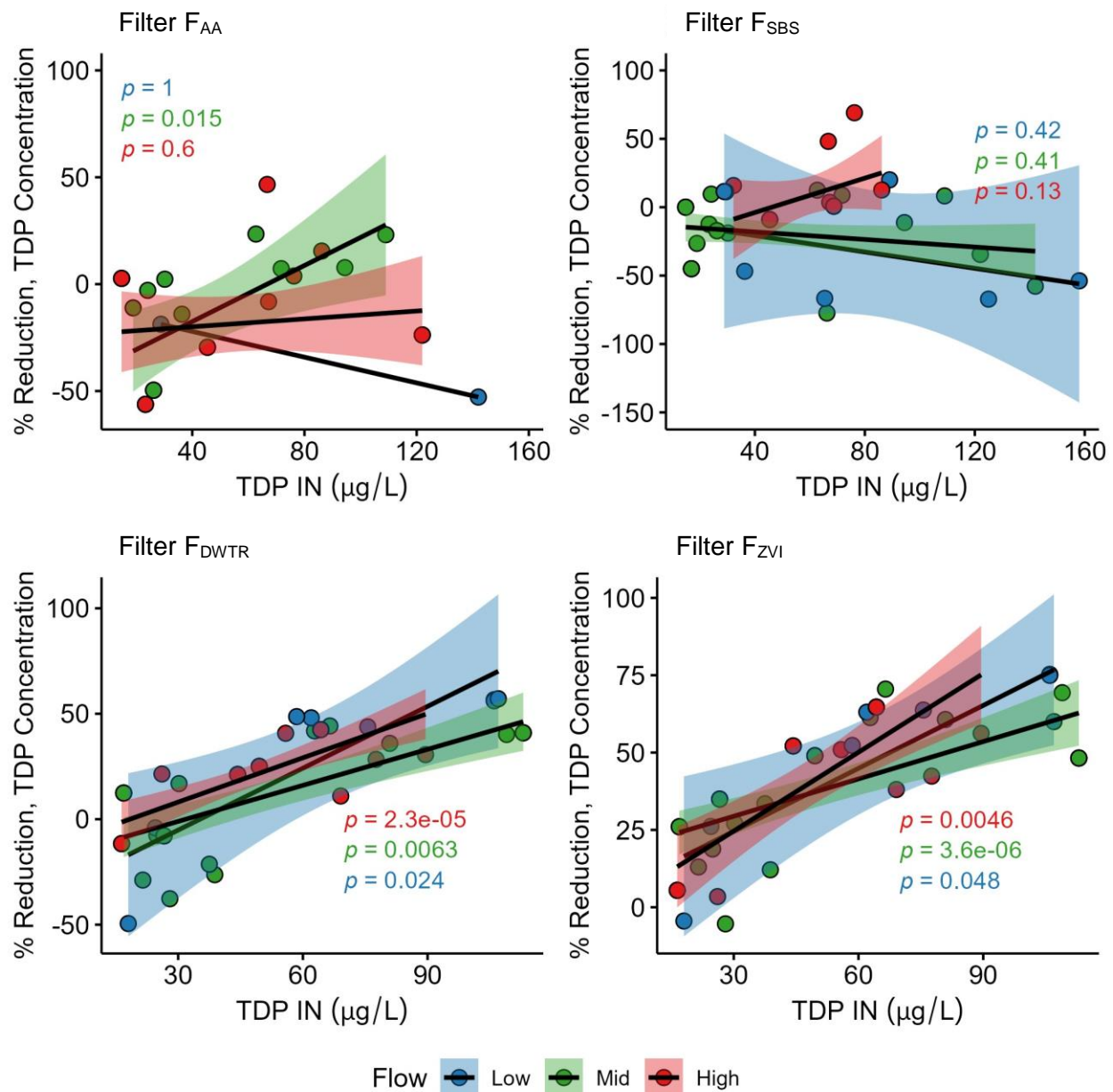


Figure 28. Percent reduction of inflow TDP concentrations grouped by flow strata

5.2.5. Cumulative TP and TDP flux over the monitoring period

We used cumulative filter outflow volumes and concentration data from grab samples collected roughly weekly to estimate cumulative P flux in the filter inflows and outflows. Our estimation method was as follows:

1. For each sampling date, P concentrations in samples collected in the current week were averaged with those collected the previous week.

2. The elapsed flow volume at each filter outflow between the previous sampling date and the current sampling date was calculated.
3. P concentrations averaged from successive sampling dates (from step 1) were multiplied by the elapsed flow volume occurring between the sampling dates/times (from step 2) to estimate the P flux occurring over the ~week-long period between sampling dates/times.
4. The “interval” P flux estimates from step 3 were summed for each filter to estimate the P flux over the monitoring period.

Estimated TP and TDP fluxes in inflows and outflows for each filter are provided in Table 16. Given the many invalid TDP results at F_{AA} , the F_{AA} outflow P flux was not calculated.

Table 16. P flux in filter inflows and outflows

Filter	TP				TDP			
	Inflow (g)	Outflow (g)	Reduction (g)	Reduction (%)	Inflow (g)	Outflow (g)	Reduction (g)	Reduction (%)
F_{AA}	876	660	216	25	480	NA	NA	NA
F_{SBS}	689	731	-42	-6	383	427	-43	-11
F_{DWTR}	311	225	86	28	183	149	34	19
F_{ZVI}	170	103	67	40	100	56	44	44

P flux percent reduction estimates in Table 16 compare reasonably well with percent load reduction estimates calculated from regression line slopes (Table 15). For F_{DWTR} and F_{ZVI} , the P flux percent reduction estimates in Table 16 are somewhat lower for TP and higher for TDP than the corresponding load reductions in Table 15. Although the F_{DWTR} TP reduction (28%) was lower than for F_{ZVI} (40%), F_{DWTR} reduced more TP (86 g) than F_{ZVI} (67 g) due to higher treated volume. Note, however, that despite reasonably consistent P concentration reductions at F_{DWTR} , P load reductions were not statistically significant (Table 13).

In Table 16, both the percent reductions and the P mass reduced were lower than we had expected to find. We expected to find significant and substantial reductions in P concentrations and loads at all four filters. Given the demonstrated dependence of P concentration reduction on inflow P concentration, the relatively low P concentrations in the inflow (~95 µg/L TP, ~60 µg/L TDP), combined with lower-than-expected treated water volumes at F_{DWTR} and F_{ZVI} , explain the modest P flux reductions at these filters. For comparison, the total flow volumes passing F_{AA} were more than twice as high as at F_{DWTR} and four times higher than at F_{ZVI} .

5.3. P Reduction Crediting

Since we lack long-term performance data, we must extrapolate from this ~8-month dataset and apply an approximate longevity estimate. Over a 10-year period F_{DWTR} and F_{ZVI} should remove between 0.7 and 0.9 kg of TP. This approximation does not account for additional treated flows outside the ~8-month monitoring period, inter-annual variability in P concentrations and loads, or diminishment of P sorption capacity over the period. Note, again, that TP and TDP load reductions at F_{DWTR} were not significant by the Wilcoxon rank sum test (Table 13).

It should be possible to make reasonable extrapolations from these filter performance data to the scale of an entire stormwater pond based on the 9.5 ft. width (axis parallel to the pond edge) of the filter cells. Per foot of filter width, Filter C should reduce 0.09 kg TP/ft. and Filter D should reduce 0.07 kg TP/ft. over a 10-year period. The Dorset Park stormwater pond has a perimeter of approximately 650 feet. If the entire pond was ringed with P filters, the theoretical P removal could be 59 kg P for DWTR filters (F_{DWTR}) or 46 kg P for ZVI filters (F_{ZVI}), assuming inflows were adequate.

The total construction costs of F_{DWTR} and F_{ZVI} were \$5,700 and \$7,200, respectively. The filters should not require maintenance other than periodically removing debris from the intake pipes. Therefore, over a 10-year period the cost of P removal should be ~\$7,000 per kg P for DWTR filters and ~\$11,000 per kg P for F_{ZVI} filters.

5.4. P Filter Design Improvements

Based on the results of this study, there are some refinements we recommend when siting, designing, and constructing P filters to treat stormwater pond outflow:

1. Sizing the filter outlet pipe down at the monitoring manhole from 4-inch diameter SDR35 pipe to 2"-PVC pipe and creating a pipe trap was for the sole purpose of low flow measurement. From a filter performance standpoint, the increased pipe friction and complexity are counterproductive. If continuous flow measurement is not needed, filter outflows should be piped straight to the pond outlet structure. Also, multiple filter cells could be connected to a common outlet pipe.
2. The type of activated alumina granules used in F_{AA} (Delta Adsorbents F-200 3/16" inch diameter) did not perform well. While some reduction of TP was suggested by comparison of inflow and outflow concentrations, this was not statistically significant. Further, F_{AA} did significantly decrease the pH to unacceptable levels. Also, given the recurrent problems in the TDP analyses of F_{AA} outflow samples, which we suspect are related to an unknown interference (possibly aluminum), we also have concerns regarding aluminum release from the media. In May 2023, we attempted to evaluate this possibility by analyzing an F_{AA} outflow sample for metals; however, the filters were not flowing. Instead, we capped the F_{AA} outlet pipe out of an abundance of caution. There are other activated alumina products available that are more commonly used in P filter applications (such as AA400G) that likely sorb P more efficiently than 3/16" F-200. However, we believe the hydraulic conductivity of these alternate materials would be too low to pass high stormwater pond outflows (the granules are too small). Therefore, we do not recommend activated alumina for stormwater pond P filters.

5.5. Recommendations Regarding Implementation of P Filter Retrofits

Water quality data are lacking for stormwater ponds in the Lake Champlain Basin. The grab samples Stone collected from 10 South Burlington stormwater ponds on November 13, 2020 under low flow conditions had a mean TDP concentration of only 31 $\mu\text{g/L}$ (Appendix B). We found a slightly higher mean TDP concentration, 41 $\mu\text{g/L}$, when we resampled a subset of these ponds on December 25, 2020, under high flow conditions. On both dates the mean TDP concentration was well below the 60 $\mu\text{g/L}$ median value reported in the International Best Management Practices Database (Clary et al, 2017). On December 25, 2020, the 60 $\mu\text{g/L}$

median value was exceeded only at the Dorset Park (62 µg/L) and South Pointe 2 (64 µg/L) stormwater ponds, and then only slightly. These results likely underestimate annual average TDP concentrations, because no samples were collected in the summer months, when we measured the highest TDP concentrations at the Dorset Park stormwater pond (summer median = ~83 µg/L). Note that over the 8-month monitoring period in the Dorset Park stormwater pond we measured median TP and TDP concentrations of 95 µg/L and 60 µg/L, nearly identical to the median P concentrations (90 µg/L and 60 µg/L, respectively) reported in Clary et al. (2017).

Considering that P removal efficiency is a function of inflow P concentration, there is little value in treating flows with very low dissolved P concentration. In this study we found reasonably good dissolved P reduction—69% for DWTR and 44% for ZVI—at an inflow TDP concentration of 60 µg/L. For the purpose of screening stormwater ponds for suitability for installation of P filter retrofits, we consider ~60 µg/L to be a reasonable TDP concentration cutoff below which implementation of P filters may not be warranted.

As we designed the P filters for this study, the configuration of the outlet structure was of primary importance. Unless an entirely different outlet is constructed from the pond (a major undertaking), the filter outlet needs to be installed below the elevation of the lowest orifice in the outlet structure. This allows installation of the treated water collection pipe slightly below the elevation of the “permanent” pool surface. The elevation difference between the surface of the pond and the outflow in the collection pipe causes the filter to flow. Four or five of the 11 ponds we sampled in South Burlington do not have suitable outlet structures. At three of these the outlets were simply horizontal culverts installed through the pond embankment. This type of pond outlet is not suitable for a P filter retrofit with gravity flow because it is not possible to install the filter collection pipe and outlet at a lower elevation.

Other siting considerations include access for heavy machinery and the dimensions of the embankment. As a general recommendation, filters should be installed in the pond bank excavated in the surrounding ground, not in an embankment. A structural engineer may be needed to review engineering plans if filter installation is proposed in a stormwater pond embankment.

It is not possible for Stone to estimate the effective lifespan of a filter or the filter media with confidence. To our knowledge the design of the filters installed at the Dorset Park stormwater pond are unique. We lack experience with them beyond the term of the study. The main factors that limit the lifespan of a P filter are clogging and reduced P sorption capacity of the media. In the Dorset Park project, Stone attempted to maximize the longevity of the filters by using large quantities of highly conductive media. A greater quantity of media will bind more P over a longer period and will be less likely to clog. The main drawback of this approach is that it is not feasible to replace the large quantity of media without essentially reconstructing the filter.

Similarly, Stone’s view regarding the eventual fate of the P filters is that they should be allowed to operate until they cease to remove P, at which time the outlet pipes may be capped. As the filters consist of crushed stone and a benign amendment buried in the bank, we believe they can remain in place indefinitely. Note that Stone will revisit questions concerning the ultimate fate of the P filters as part of the ongoing Lake Carmi tile drain P filter study, in consultation with Vermont Department of Environmental Conservation and Vermont Agency of Agriculture, Food & Markets staff.

6. Conclusions

Stone designed and constructed media filters to remove P from stormwater pond outflow, a challenging application. The hydraulic design of these filters was generally successful, proving the concept. Although the filter containing DWTR did significantly reduce TP and TDP concentrations, the filter containing ZVI performed better (~52% reduction in TP and TDP concentrations) than the other three filters. P concentration reduction was strongly dependent on inflow P concentration. Relatively low P concentrations in the inflow (median ~95 µg/L TP and ~60 µg/L TDP) resulted in somewhat lower P concentration reduction efficiency than we were expecting. Based on these results, we recommend use of ZVI in similar P filter applications. We recommend against using activated alumina, which performed poorly and significantly depressed pH.

7. Deliverables Completed

Stone prepared quarterly progress reports within 10 days following the end of each calendar quarter. These quarterly reports provided updates on the progress of each task and described any problems encountered.

Stone prepared an interim report following completion of Task 2 of the workplan, the stormwater pond evaluation. This interim report is included as Appendix B. Another interim deliverable was the as-built P filter plans included as Appendix C.

This final report includes methods and results of the stormwater pond P filter evaluation.

Stone presented aspects of the stormwater pond P filter design and construction at the following meetings:

- LCBP Technical Advisory Committee (TAC) on February 1, 2023
- Vermont Agricultural Water Quality Partnership, Scientific Advisory Committee, May 2, 2022

This final report was presented to the LCBP TAC on September 6, 2023.

8. References

- Belden, B.S., and B. Fossum. 2018. Iron Enhanced Sand Filter Performance for Reducing Phosphorus from a Regional Stormwater Pond. World Environmental and Water Resources Congress 2018. Url: <https://ascelibrary.org/doi/10.1061/9780784481431.007>.
- Braun, D.C. 2023. Assessment of Tile Drainage Systems in Addison County and the Jewett Brook Watershed. Technical Report No. 104. Lake Champlain Basin Program, Grand Isle, VT. URL: https://www.lcbp.org/wp-content/uploads/2016/03/104_Assessment-of-Tile-Drainage-Systems-in-Addison-County-and-the-Jewett-Brook-Watershed.pdf (Accessed 6-23-2023).
- Braun, D.C. 2017. End-of-Tile Phosphorous Removal System Project: Final Report. Prepared for Vermont USDA NRCS, Colchester, VT.
- Bryant, R.B., A.R. Buda, P.J.A. Kleinman, C.D. Church, L.S. Saporito, G.J. Folmar, S. Bose, and A.L. Allen. 2012. Using flue gas desulfurization gypsum to remove dissolved phosphorus from agricultural drainage waters. *J. Environ. Qual.* 41:664-671.
- Clary, J., J. Jones, M. Leisenring, P. Hobson, and E. Strecker. 2017. International Stormwater BMP Database, 2016 Summary Statistics. Prepared for the Water Environment and Reuse Foundation, Alexandria, VA.
- Dressing, S.A., D.W. Meals, J.B. Harcum, J. Spooner, J.B. Stribling, R.P. Richards, C.J. Millard, S.A. Lanberg, and J.G. O'Donnell. 2016. Monitoring and Evaluating Nonpoint Source Watershed Projects. EPA 841-R-16-010. USEPA, Washington, DC.
- Gulliver, J.S. 2018. When Retention Ponds are a Source of Phosphorus. Presentation to Minnesota Cities Stormwater Coalition, July 19, 2018.
- McDowell, R.W., A.N. Sharpley, and W. Bourke. 2008. Treatment of drainage water with industrial by-products to prevent phosphorus loss from tile-drained land. *J. Environ. Qual.* 37:1575–1582.
- Penn, C.J., J.M. McGrath, E. Rounds, G. Fox, and D. Heeren. 2012. Trapping phosphorus in runoff with a phosphorus removal structure. *J. Environ. Qual.* 41:672-679.
- Vermont Agency of Natural Resources. 2022. Vermont Water Quality Standards 2022. URL: <https://dec.vermont.gov/sites/dec/files/documents/2022-Vermont-Water-Quality-Standards.pdf> (Accessed 6-23-2023).
- Vermont Agency of Natural Resources. 2017. 2017 Vermont Stormwater Management Manual Rule and Design Guidance. Montpelier, VT. URL:

https://dec.vermont.gov/sites/dec/files/wsm/stormwater/docs/Permitinformation/2017%20VSMM_Rule_and_Design_Guidance_04172017.pdf (Accessed 6-23-2023).

Vermont Agriculture and Environmental Laboratory. 2020. Quality Systems Manual, Revision No. 25. Randolph Center, VT. URL:

<https://agriculture.vermont.gov/sites/agriculture/files/documents/VAEL/QA-001.26%20VAEL%20QSM%20Uncontrolled.pdf> (Accessed 6-23-2023).

Appendix A: Quality Assurance Project Plan

Appendix B: Interim Report on Stormwater Pond Evaluation

Appendix C: As-Built P Filter Drawings

Appendix D: Flow and Water Quality Monitoring Data

Date	Structure	TDP (µg P/L)	TP (µg P/L)	Flow Total Begin (L)	Flow Total End (L)	Elapsed Flow (L)	Flow Rate (L/min)	TDP Load (mg P/hr)	TP Load (mg P/hr)	VAEL Remarks	Comments
3/18/2022	IN1	42.8	56.7								
3/24/2022	IN1	30.2	41.4								
4/1/2022	IN1	19.7	37.0								
4/1/2022	IN1 dupe	18.1	36.3								
4/8/2022	IN1	66.7	144								
4/14/2022	IN1	16.9	32.6								
4/21/2022	IN1	32.2	40.4								
4/28/2022	IN1	14.8	27.1								
5/5/2022	IN1	29.4	45.4								
5/13/2022	IN1	91.6	144								
5/13/2022	IN1 dupe	86.4	145								
5/17/2022	IN1	109	191								
5/27/2022	IN1	71.7	103								
6/3/2022	IN1	97.2	137								
6/3/2022	IN1 dupe	91.6	142								
6/10/2022	IN1	62.7	83.8								
6/16/2022	IN1	100	191								
6/23/2022	IN1	66.2	133								
7/1/2022	IN1	158	223								
7/7/2022	IN1	125	201								
7/20/2022	IN1	122	432								
7/29/2022	IN1	76.2	140								
8/6/2022	IN1	142	258								
8/13/2022	IN1	65.4	91.6							TP=E (estimated)	
8/31/2022	IN1	45.4	76.6							TDP=E (estimated), LCSL failed criteria	
9/14/2022	IN1	83.1	123								
9/14/2022	IN1 dupe	89.2	124								
9/20/2022	IN1	67.2	79.3								
9/29/2022	IN1	23.3	36.0								
10/5/2022	IN1	20.4	20.0								
10/20/2022	IN1	24.1	25.7								
10/27/2022	IN1	36.3	113								
11/10/2022	IN1	28.8	160								
11/18/2022	IN1	26.2	43.0								
11/28/2022	IN1	68.7	99.6								

Date	Structure	TDP (µg P/L)	TP (µg P/L)	Flow Total Begin (L)	Flow Total End (L)	Elapsed Flow (L)	Flow Rate (L/min)	TDP Load (mg P/hr)	TP Load (mg P/hr)	VAEL Remarks	Comments
12/8/2022	IN1	46.7	92.6								
12/15/2022	IN1	27.5	invalid								Invalid TP--Kip broke through ice, muddied pond
3/18/2022	IN2	38.8	55.1								
3/24/2022	IN2	28.0	53.7								
4/1/2022	IN2	21.5	43.7								
4/8/2022	IN2	55.6	95.3								
4/8/2022	IN2 dupe	56.1	93.8								
4/14/2022	IN2	16.4	25.9								
4/21/2022	IN2	28.6	37.4								
4/21/2022	IN2 dupe	23.6	37.7								
4/28/2022	IN2	16.9	26.4								
5/5/2022	IN2	30.2	45.8								
5/13/2022	IN2	75.6	156								
5/17/2022	IN2	109	166								
5/27/2022	IN2	66.5	93.5								
6/3/2022	IN2	80.9	126								
6/10/2022	IN2	60.4	92.2								
6/10/2022	IN2 dupe	65.2	92.2								
6/16/2022	IN2	65.3	155								
6/23/2022	IN2	62.0	140								
7/1/2022	IN2	106	195								
7/7/2022	IN2	106	182								
7/20/2022	IN2	106	269								
7/20/2022	IN2 dupe	120	282								
7/29/2022	IN2	77.6	138								
8/6/2022	IN2	107	144								
8/13/2022	IN2	58.5	80.6							TP=E (estimated)	
8/31/2022	IN2	49.5	82.5							TDP=E (estimated), LCSL failed criteria	
9/14/2022	IN2	89.5	122								
9/20/2022	IN2	68.4	77.6								
9/20/2022	IN2 dupe	69.8	82.0								
9/29/2022	IN2	24.9	27.4								
10/5/2022	IN2	14.1	18.9								
10/20/2022	IN2	18.0	35.0								

Date	Structure	TDP (µg P/L)	TP (µg P/L)	Flow Total Begin (L)	Flow Total End (L)	Elapsed Flow (L)	Flow Rate (L/min)	TDP Load (mg P/hr)	TP Load (mg P/hr)	VAEL Remarks	Comments
10/27/2022	IN2	37.5	123								
11/10/2022	IN2	24.5	169								
11/18/2022	IN2	26.4	49.4								
11/18/2022	IN2 dupe	26.8	51.6								
11/28/2022	IN2	64.3	89.6								
12/8/2022	IN2	44.3	67.6								
12/15/2022	IN2	22.5	invalid								Invalid TP--Kip broke through ice, muddied pond
3/18/2022	F _{AA}	invalid	49.6	155,173.5	NA	NA	29.6	invalid	88	confirmed DP > TP	Invalid TDP
3/24/2022	F _{AA}	29.5	40.6	313,339.7	314,548.4	1208.7	22.0	39	54		
4/1/2022	F _{AA}	21.0	34.6	540,920.2	541,862.0	941.8	15.7	20	33		
4/8/2022	F _{AA}	35.6	61.6	695,220.0	697,813.4	2593.4	66.5	142	246		
4/14/2022	F _{AA}	invalid	37.8	1,059,066.2	1,060,533.8	1467.6	31.2	invalid	71		Invalid TDP
4/14/2022	F _{AA} dupe	invalid	36.6	1,059,066.2	1,060,533.8	1467.6	31.2	invalid	69		Invalid TDP
4/21/2022	F _{AA}	invalid	32.3	1,443,621.0	1,446,064.0	2443.0	54.3	invalid	105		Invalid TDP
4/28/2022	F _{AA}	14.4	21.0	1,825,773.4	1,826,993.4	1220.0	33.0	28	42		
5/5/2022	F _{AA}	invalid	28.6	2,043,925.0	2,044,873.0	948.0	20.2	invalid	35	confirmed DP > TP	Invalid TDP
5/13/2022	F _{AA}	invalid	86.9	2,208,867.0	2,209,374.0	507.0	9.1	invalid	47		Invalid TDP
5/17/2022	F _{AA}	invalid	136	2,270,979.0	2,271,938.0	959.0	16.5	invalid	135	TDP = E (estimated)	VAEL estimated TDP--use dupe instead
5/17/2022	F _{AA} dupe	83.8	138	2,270,979.0	2,271,938.0	959.0	16.5	83	137		
5/27/2022	F _{AA}	66.5	69.2	2,610,170.0	2,611,477.0	1307.0	22.9	91	95		
6/3/2022	F _{AA}	87.1	84.5	2,781,981.0	2,783,137.0	1156.0	19.6	102	99		
6/10/2022	F _{AA}	48.0	46.8	2,958,456.0	2,959,484.0	1028.0	23.9	69	67		
6/16/2022	F _{AA}	invalid	338	3,126,053.0	3,126,809.0	756.0	13.3	invalid	269		Invalid TDP
6/16/2022	F _{AA} dupe	invalid	163	3,126,053.0	3,126,809.0	756.0	13.3	invalid	130		Invalid TDP
6/23/2022	F _{AA}	invalid	94.4	3,246,849.9	3,247,570.3	720.4	18.47	invalid	105		Invalid TDP
7/1/2022	F _{AA}	invalid	233	3,541,329.2	3,542,123.0	793.8	15.27	invalid	213		Invalid TDP
7/7/2022	F _{AA}	invalid	264	3,681,096.4	3,681,694.5	598.1	13.59	invalid	215		Invalid TDP
7/20/2022	F _{AA}	151	189	3,930,927.6	3,932,883.5	1955.9	35.56	322	403		
7/29/2022	F _{AA}	74.0	112	4,226,077.2	4,231,340.5	5263.2	93.99	417	632		
7/29/2022	F _{AA} dupe	72.6	112	4,226,077.2	4,231,340.5	5263.2	93.99	409	632		
8/6/2022	F _{AA}	217	267	4,407,039.6	4,407,533.6	494.0	9.50	124	152		
8/13/2022	F _{AA}	invalid	136	4,564,467.3	4,565,023.8	556.5	10.70	invalid	87	TP=E (estimated)	Invalid TDP
8/31/2022	F _{AA}	58.8	65.1	4,842,133.0	4,843,805.0	1672.0	35.57	126	139	TDP=E (estimated), LCSL failed criteria	

Date	Structure	TDP (µg P/L)	TP (µg P/L)	Flow Total Begin (L)	Flow Total End (L)	Elapsed Flow (L)	Flow Rate (L/min)	TDP Load (mg P/hr)	TP Load (mg P/hr)	VAEL Remarks	Comments
9/14/2022	F _{AA}	72.8	94.6	5,061,352.2	5,067,271.1	5918.9	128.67	562	730		
9/20/2022	F _{AA}	72.7	68.2	5,576,974.5	5,586,160.6	9186.1	153.10	668	626		
9/29/2022	F _{AA}	invalid	27.1	6,303,142.9	6,304,918.7	1775.7	34.15	invalid	56	TDP=E (estimated)	VAEL estimated TDP--use dupe instead
9/29/2022	F _{AA} dupe	36.4	26.3	6,303,142.9	6,304,918.7	1775.7	34.15	75	54		
10/5/2022	F _{AA}	invalid	30.0	6,458,975.4	6,459,428.9	453.5	6.48	invalid	11.7		Invalid TDP
10/20/2022	F _{AA}	24.8	23.2	7,048,529.9	7,049,530.0	1000.1	21.28	31.7	29.6		
10/27/2022	F _{AA}	41.4	95.4	7,221,570.1	7,222,714.5	1144.3	20.08	50	115		
11/10/2022	F _{AA}	34.2	46.0	7,521,723.7	7,522,488.8	765.0	12.97	26.6	35.8		
11/18/2022	F _{AA}	39.2	36.0	7,989,853.9	7,990,706.7	852.9	19.38	46	42		
11/28/2022	F _{AA}	invalid	49.3	8,144,784.7	8,146,142.6	1357.8	27.16	invalid	80		Invalid TDP
11/28/2022	F _{AA} dupe	invalid	47.0	8,144,784.7	8,146,142.6	1357.8	27.16	invalid	77		Invalid TDP
12/8/2022	F _{AA}	invalid	invalid	8,451,341.4	8,452,573.2	1231.8	29.33	invalid	invalid		Invalid TDP and TP
12/15/2022	F _{AA}	36.4	32.2	8,586,405.6	8,586,748.2	342.6	7.61	16.6	14.7		
3/18/2022	F _{SBS}	invalid	63.9	139,204.7	NA	NA	17.7	invalid	68	confirmed DP > TP	Invalid TDP
3/24/2022	F _{SBS}	35.9	43.8	258,643.6	260,062.3	1418.7	25.8	56	68		Switched begin and end flow totals
4/1/2022	F _{SBS}	23.9	39.1	432,674.1	433,477.7	803.6	13.4	19	31		
4/8/2022	F _{SBS}	34.6	58.7	582,767.2	585,017.6	2250.4	57.7	120	203		
4/14/2022	F _{SBS}	24.5	36.1	912,002.6	913,286.2	1283.6	27.3	40	59		
4/21/2022	F _{SBS}	27.1	29.5	1,247,909.0	1,249,972.0	2063.0	45.8	75	81		
4/28/2022	F _{SBS}	14.8	22.3	1,549,163.5	1,549,992.1	828.6	21.2	19	28		
5/5/2022	F _{SBS}	invalid	28.3	1,707,745.0	1,708,391.0	646.0	13.5	invalid	23	confirmed DP > TP	Invalid TDP--use dupe value instead
5/5/2022	F _{SBS} dupe	26.1	29.9	1,707,745.0	1,708,391.0	646.0	13.5	21	24		
5/13/2022	F _{SBS}	71.2	92.5	1,811,722.0	1,811,918.0	196.0	3.5	15	19		
5/17/2022	F _{SBS}	100	136	1,844,329.0	1,845,260.0	931.0	15.5	93	127		
5/27/2022	F _{SBS}	65.4	84.1	2,073,702.0	2,074,427.0	725.0	12.5	49	63		
6/3/2022	F _{SBS}	105	649	2,182,158.0	2,182,946.0	788.0	13.4	84	520		
6/10/2022	F _{SBS}	54.9	206	2,293,456.0	2,294,189.0	733.0	17.5	57	216		
6/16/2022	F _{SBS}	201	897	2,415,972.8	2,416,338.5	365.7	6.3	76	339		
6/23/2022	F _{SBS}	135	157	2,472,549.2	2,472,991.7	442.5	11.06	90	104		Poor TP and TDP dupes, but keep data
6/23/2022	F _{SBS} dupe	99.8	228	2,472,549.2	2,472,991.7	442.5	11.06	66	151		Poor TP and TDP dupes, but keep data
7/1/2022	F _{SBS}	243	266	2,644,170.3	2,644,517.4	347.1	6.55	95	105		
7/7/2022	F _{SBS}	209	288	2,727,100.4	2,727,411.1	310.8	7.06	89	122		

Date	Structure	TDP (µg P/L)	TP (µg P/L)	Flow Total Begin (L)	Flow Total End (L)	Elapsed Flow (L)	Flow Rate (L/min)	TDP Load (mg P/hr)	TP Load (mg P/hr)	VAEL Remarks	Comments
7/20/2022	F _{SBS}	164	320	2,848,090.1	2,848,879.0	788.9	14.34	141	275		
7/29/2022	F _{SBS}	23.6	122	3,026,046.4	3,030,016.2	3969.8	70.89	100	519		
8/6/2022	F _{SBS}	224	283	3,136,226.2	3,136,704.6	478.5	9.20	124	156	TP=I (matrix interference)	
8/6/2022	F _{SBS} dupe	224	285	3,136,226.2	3,136,704.6	478.5	9.20	124	157		
8/13/2022	F _{SBS}	109	127	3,290,960.9	3,291,363.7	402.8	7.75	51	59	TP=E (estimated)	
8/31/2022	F _{SBS}	49.5	60.4	3,537,685.4	3,539,321.0	1635.7	35.56	106	129	TDP=E (estimated), LCSL failed criteria	
9/14/2022	F _{SBS}	75.3	108	3,739,620.4	3,745,655.9	6035.5	131.21	593	850		
9/20/2022	F _{SBS}	64.8	68.5	4,221,418.9	4,231,003.2	9584.3	162.45	632	668		
9/29/2022	F _{SBS}	26.2	25.6	4,887,826.7	4,889,366.6	1539.9	30.19	47	46		
10/5/2022	F _{SBS}	37.9	54.2	4,970,616.3	4,970,616.6	0.379	0.005	0.0	0.0		
10/5/2022	F _{SBS} dupe	35.0	42.9	4,970,616.3	4,970,616.6	0.379	0.005	0.0	0.0		
10/20/2022	F _{SBS}	21.8	27.9	5,422,932.8	5,423,392.4	459.5	9.78	12.8	16.4		
10/27/2022	F _{SBS}	53.3	108	5,485,761.2	5,486,242.0	480.7	8.58	27.5	56		
11/10/2022	F _{SBS}	25.5	48.3	5,679,373.3	5,679,750.3	377.0	6.28	9.6	18.2		
11/18/2022	F _{SBS}	30.7	38.7	6,191,196.9	6,192,574.8	1377.9	30.62	56	71		
11/28/2022	F _{SBS}	68.2	112	6,480,963.4	6,483,444.0	2480.6	50.62	207	340		Suspect TDP and TP switched (corrected)
12/8/2022	F _{SBS}	invalid	invalid	7,002,963.3	7,004,750.1	1786.7	43.58	invalid	invalid	TDP=I (matrix interference)	Suspect bottle switch, invalid TDP--use dupe instead
12/8/2022	F _{SBS} dupe	38.7	56.8	7,002,963.3	7,004,750.1	1786.7	43.58	101	173		
12/15/2022	F _{SBS}	26.2	66.0	7,259,493.5	7,260,184.7	691.2	15.03	23.6	60		
3/18/2022	F _{DWTR}	49.0	58.4	NA	NA	NA	12.3	36	43		F _{DWTR} flowmeter not recording
3/24/2022	F _{DWTR}	35.0	40.8	51,796.2	52,287.5	491.3	8.9	19	22		
3/24/2022	F _{DWTR} dupe	42.1	54.0	51,796.2	52,287.5	491.3	8.9	23	29		
4/1/2022	F _{DWTR}	27.7	32.7	122,030.7	122,252.9	222.2	3.7	6.2	7.3		
4/8/2022	F _{DWTR}	33.1	59.0	164,925.8	167,027.1	2101.3	53.9	107	191		
4/14/2022	F _{DWTR}	18.3	28.3	416,715.2	417,599.8	884.6	18.4	20	31		
4/21/2022	F _{DWTR}	20.5	27.9	655,675.3	657,255.0	1579.7	35.1	43	59		
4/28/2022	F _{DWTR}	14.7	22.5	834,503.5	834,862.0	358.5	9.4	8.3	13		
4/28/2022	F _{DWTR} dupe	14.9	23.0	834,503.5	834,862.0	358.5	9.4	8.4	13		
5/5/2022	F _{DWTR}	25.1	30.4	889,248.9	889,482.4	233.5	5.0	7.5	9.1		
5/13/2022	F _{DWTR}	42.5	60.2	931,261.6	931,346.8	85.2	1.5	3.9	5.5		
5/17/2022	F _{DWTR}	65.2	82.6	942,105.0	942,441.1	336.1	5.7	22	28		
5/27/2022	F _{DWTR}	37.1	49.7	1,051,631.4	1,051,914.1	282.7	5.0	11	15	TDP = E (estimated)	

Date	Structure	TDP (µg P/L)	TP (µg P/L)	Flow Total Begin (L)	Flow Total End (L)	Elapsed Flow (L)	Flow Rate (L/min)	TDP Load (mg P/hr)	TP Load (mg P/hr)	VAEL Remarks	Comments
6/3/2022	F _{DWTR}	51.8	61.5	1,100,919.0	1,101,134.0	215.0	3.7	12	14		
6/10/2022	F _{DWTR}	36.5	66.3	1,137,455.0	1,137,648.0	193.0	4.4	10	17		
6/16/2022	F _{DWTR}	58.6	302	1,149,822.7	1,149,823.4	0.7	0.012	0.0	0.2		
6/23/2022	F _{DWTR}	32.2	31.8	1,152,595.4	1,152,659.8	64.4	1.65	3.2	3.1		
7/1/2022	F _{DWTR}	52.7	134	1,183,986.0	1,183,987.5	1.5	0.029	0.1	0.2		Poor TP and TDP dupes, but keep data
7/1/2022	F _{DWTR} dupe	39.2	73.6	1,183,986.0	1,183,987.5	1.5	0.029	0.1	0.1		Poor TP and TDP dupes, but keep data
7/7/2022	F _{DWTR}	46.5	98.2	1,196,678.8	1,196,716.3	37.5	0.85	2.4	5.0		Suspect TDP and TP switched (corrected)
7/20/2022	F _{DWTR}	66.7	150	1,250,750.8	1,250,957.5	206.7	3.76	15.0	33.8		
7/29/2022	F _{DWTR}	55.6	123	1,339,486.9	1,341,750.6	2263.7	41.16	137.3	304		
8/6/2022	F _{DWTR}	45.9	60.6	1,372,239.4	1,372,241.7	2.3	0.044	0.1	0.2		
8/13/2022	F _{DWTR}	30.6	invalid	1,441,442.8	1,441,476.9	34.1	0.66	1.2	invalid	TP=E (estimated)	VAEL estimated TP--use dupe instead
8/13/2022	F _{DWTR} dupe	29.5	42.7	1,441,442.8	1,441,476.9	34.1	0.66	1.2	1.7		
8/31/2022	F _{DWTR}	37.1	49.7	1,574,353.1	1,574,978.9	625.7	13.60	30.3	41	TDP=E (estimated), LCSL failed criteria	
9/14/2022	F _{DWTR}	62.1	92.4	1,730,752.0	1,735,206.6	4454.7	96.84	361	537		
9/20/2022	F _{DWTR}	61.5	70.2	2,080,202.6	2,087,893.5	7690.8	130.35	481	549		
9/29/2022	F _{DWTR}	26.8	27.9	2,574,232.2	2,574,812.1	579.9	11.37	18.3	19.0		
10/5/2022	F _{DWTR}	62.1	134	2,591,103.0	2,591,103.4	0.379	0.005	0.0	0.0		
10/20/2022	F _{DWTR}	26.4	36.9	2,899,342.3	2,899,394.1	51.9	1.10	1.7	2.4		
10/20/2022	F _{DWTR} dupe	27.4	33.9	2,899,342.3	2,899,394.1	51.9	1.10	1.8	2.2		
10/27/2022	F _{DWTR}	45.5	61.8	2,904,445.4	2,904,496.1	50.7	0.89	2.4	3.3		
11/10/2022	F _{DWTR}	25.5	62.6	3,020,925.2	3,020,947.9	22.7	0.38	0.6	1.4		
11/18/2022	F _{DWTR}	28.7	38.3	3,329,136.0	3,329,702.3	566.3	12.87	22.2	29.6		
11/28/2022	F _{DWTR}	37.0	54.6	3,440,937.4	3,441,990.1	1052.7	21.05	47	69		Suspect TDP and TP switched (corrected)
12/8/2022	F _{DWTR}	34.9	53.4	3,744,365.4	3,745,506.7	1141.3	27.84	58	49		
12/15/2022	F _{DWTR}	21.4	29.2	3,876,022.4	3,876,327.2	304.7	6.77	8.7	11.9		
12/15/2022	F _{DWTR} dupe	22.3	27.9	3,876,022.4	3,876,327.2	304.7	6.77	9.1	11.3		
3/18/2022	F _{ZVI}	31.2	47.2	21,810.8	NA	NA	6.4	12	18		
3/18/2022	F _{ZVI} dupe	37.0	44.9	21,810.8	NA	NA	6.4	14	17		
3/24/2022	F _{ZVI}	29.5	41.8	47,108.3	47,376.3	268.0	4.9	8.6	12		
4/1/2022	F _{ZVI}	18.7	26.5	84,456.3	84,568.0	111.7	1.9	2.1	3.0		

Date	Structure	TDP (µg P/L)	TP (µg P/L)	Flow Total Begin (L)	Flow Total End (L)	Elapsed Flow (L)	Flow Rate (L/min)	TDP Load (mg P/hr)	TP Load (mg P/hr)	VAEL Remarks	Comments
4/8/2022	F _{ZVI}	27.4	57.0	111,908.9	113,279.2	1370.3	36.1	59	123		
4/14/2022	F _{ZVI}	15.5	27.4	247,954.3	248,361.6	407.3	8.3	7.7	13.7		Suspect TDP and TP switched (corrected)
4/21/2022	F _{ZVI}	25.2	25.7	381,233.4	382,122.6	889.2	19.8	30	30		
4/28/2022	F _{ZVI}	12.5	25.9	467,660.0	467,816.3	156.3	4.0	3.0	6.2		
5/5/2022	F _{ZVI}	22.0	29.9	494,553.5	494,660.2	106.7	2.2	2.9	4.0		
5/13/2022	F _{ZVI}	27.4	63.3	510,515.0	510,544.2	29.2	0.51	0.8	1.9		
5/17/2022	F _{ZVI}	33.4	76.5	513,092.1	513,189.8	97.7	1.6	3.3	7.5		
5/27/2022	F _{ZVI}	20.0	30.6	557,948.1	558,029.5	81.4	1.4	1.7	2.6		
5/27/2022	F _{ZVI} dupe	19.2	28.6	557,948.1	558,029.5	81.4	1.4	1.6	2.5		
6/3/2022	F _{ZVI}	31.8	69.5	575,257.7	575,338.7	81.0	1.4	2.7	5.8		
6/10/2022	F _{ZVI}	24.3	40.8	592,639.5	592,733.8	94.3	2.2	3.2	5.4		
6/16/2022	F _{ZVI}	24.3	48.9	598,852.9	598,853.7	0.8	0.014	0.0	0.0		
6/23/2022	F _{ZVI}	22.9	31.6	601,134.7	601,175.3	40.5	1.04	1.4	2.0		
7/1/2022	F _{ZVI}	26.2	33.6	625,109.3	625,110.0	0.8	0.012	0.0	0.0		
7/7/2022	F _{ZVI}	25.0	30.4	637,504.2	637,540.9	36.7	0.83	1.3	1.5		
7/7/2022	F _{ZVI} dupe	28.1	33.0	637,504.2	637,540.9	36.7	0.83	1.4	1.7		
7/20/2022	F _{ZVI}	58.5	142	692,822.3	693,107.0	284.7	5.18	18.2	44		
7/29/2022	F _{ZVI}	44.7	99.5	783,396.6	785,641.4	2244.7	40.08	108	239		
8/6/2022	F _{ZVI}	42.8	55.3	815,891.8	815,892.1	0.4	0.007	0.0	0.0		
8/13/2022	F _{ZVI}	27.9	37.1	863,320.3	863,354.4	34.1	0.66	1.1	1.5	TP=E (estimated)	
8/31/2022	F _{ZVI}	21.9	50.2	932,902.2	933,289.9	387.6	8.25	10.8	24.8	TDP=E (estimated), LCSL failed criteria	
8/31/2022	F _{ZVI} dupe	28.6	41.9	932,902.2	933,289.9	387.6	8.25	14.2	20.7	TDP=E (estimated), LCSL failed criteria	
9/14/2022	F _{ZVI}	39.2	75.7	1,026,683.9	1,029,043.8	2359.8	51.30	121	233		
9/20/2022	F _{ZVI}	42.8	51.0	1,211,351.1	1,215,052.8	3701.8	62.74	161	192		
9/29/2022	F _{ZVI}	20.2	33.6	1,457,922.6	1,458,234.1	311.5	6.11	7.4	12.3		
10/5/2022	F _{ZVI}	23.8	87.4	1,465,859.1	1,465,859.1	0.000	0.000	0.0	0.0		
10/20/2022	F _{ZVI}	18.8	26.7	1,666,775.1	1,666,797.8	22.7	0.48	0.5	0.8		
10/27/2022	F _{ZVI}	26.9	46.3	1,668,679.9	1,668,687.5	7.6	0.14	0.2	0.4		Poor TP dupe
10/27/2022	F _{ZVI} dupe	23.0	81.2	1,668,679.9	1,668,687.5	7.6	0.14	0.2	0.7		Poor TP dupe
11/10/2022	F _{ZVI}	18.1	42.8	1,716,646.4	1,716,646.4	0.000	0.000	0.0	0.0		
11/18/2022	F _{ZVI}	17.3	34.5	1,855,390.1	1,855,541.9	151.8	3.45	3.6	7.1		
11/28/2022	F _{ZVI}	22.7	41.5	1,884,282.6	1,884,732.3	449.7	8.99	12.3	22.4		
12/8/2022	F _{ZVI}	21.2	58.7	2,003,581.4	2,004,026.1	444.8	10.85	13.8	52		
12/15/2022	F _{ZVI}	13.5	79.3	2,033,716.6	2,033,748.1	31.4	0.68	0.6	3.2		

